DRAFT

Measurement of the SNO Trigger Efficiency

Josh Klein, Mark Neubauer

University of Pennsylvania

March 3, 2000

Abstract

In this report, we present an efficiency measurement for the main physics trigger of the SNO detector - the 100 ns NHIT trigger. The trigger efficiency was measured using the laserball as a source of in-time hits and FEC/D calibration channels to determine how often the trigger fires in response to these hits. It is found that the shape of the trigger efficiency is largely independent of threshold over the range of our production data taking thresholds and has an NHIT turn-on between 3.5 and 3.8 NHIT. The dependence of the efficiency on source position is found to be small within 5 m except near threshold where the efficiency is rapidly changing and the maximum difference is between 2% and 25% for the low and high NHIT thresholds, respectively. It is also determined that the medium threshold NHIT trigger (N100MED = 18.1 NHIT) is $> 99.9\%$ efficient when there are 23 or more hits within 93 ns coincidence, which implies that trigger inefficiency represents a negligible contribution to acceptance for medium to high-energy neutrino analyses in SNO. This result is found to be robust against systematic effects from timing calibrations, FEC/D charge cut positions, and modest fractions of disabled trigger channels. Two other independent methods of measuring the trigger efficiency were used as approximate checks of the results and were found to be in rough agreement with these results. In addition, the expected NHIT trigger rate based on the measured efficiency for the medium threshold trigger and PULSE_GT data was determined to be 5.5 ± 1.6 Hz, consistent with the observed rate of 6.9 ± 3 Hz over 500 hours of production neutrino data.

Contents

List of Figures

List of Tables

1 Introduction

In order to calculate the flux of neutrinos incident on SNO, one needs to connect the observed rates of various types of interactions to the probability of actually triggering the detector on the products of these interactions (e.g. e^-, n) as well as know the number of targets and the differential cross sections. These trigger probabilities are the acceptances for various types of particles produced by neutrino interactions and depend on the position, direction and energy of the particles as well as host of detector properties such as PMT efficiency/coverage, optical properties of the different media, etc. One particularly important detector property that acceptance depends upon is the trigger efficiency, which is how often the trigger hardware issues a global trigger (i.e. initiates an event) in response to a set of PMTs hit at given times. Therefore, understanding the efficiency of the trigger system is a crucial part of determining the acceptance for particles produced by neutrino interactions in the detector.

Although the trigger efficiency is an important part of any physics analysis in SNO, a knowledge of the exact shape of the efficiency curve is not necessary for all analyses. For higher energy neutrino analyses, which will dominate the early neutrino results from SNO, it may be sufficient to simply know that the trigger efficiency is very close to unity over this energy range so one does not need to worry about trigger contributions to the efficiency. However, once the data analysis in this experiment matures to the point where we are getting aggressive with our analysis threshold, the details of the trigger efficiency will be of more importance.

In addition to being crucial for data analysis, the trigger efficiency also has a profound impact on how the data is collected. In order to collect as much physics data as possible in the low end of the solar (^{8}B) neutrino spectrum (where CC spectral distortions are potentially important), we would like to set our hardware trigger threshold as low as possible. However, there is a large exponential wall of radioactive background events at low energy as well as significant contributions from random coincidences of PMT and electronics noise which ultimately limits how much we can lower our trigger threshold and still stably acquire data. While acute attention to cleanliness is what makes the level of radioactive backgrounds acceptable for analysis, the sharpness of the trigger efficiency curve is a main reason why we are able to stably trigger the detector at a very low threshold in energy (currently 5-10 Hz at 18 NHIT which is ~ 2 MeV). This is because a very sharp efficiency curve allows one to be very *efficient* at triggering on events *above* threshold while being very *inefficient* at triggering on events *below* threshold where the rate gets exponentially large.

This report is organized in the following way. A brief review of the SNO trigger system is presented in Section 2, with an emphasis placed on parts of the system critical for an understanding of the trigger efficiency measurement. In Section 3, the distinction between trigger efficiency and acceptance is reviewed and in Section 4 some of the sources of trigger inefficiency are discussed. The methods used to measure the trigger efficiency are discussed in Section 5 and the analysis results using these methods are presented in Section 6. The report is summarized in Section 7 followed by two appendices which include a discussion of error determination and some results on the 20 ns trigger efficiency.

2 The SNO Trigger System - A Brief Review

In this section, we present a brief review of the SNO trigger system, with an emphasis placed on the parts relevant to the NHIT trigger efficiency. To find more detailed information, an exhaustive description of the entire trigger system can be found in [1].

A diagram of the trigger system is shown in Figure 1. The main role of the trigger system is to determine when a potentially interesting event has occurred in the detector and then signal the front-end electronics to store any PMT data they may have accumulated. This determination is nominally based on the total number of coincident PMT hits (NHIT), but can also involve total coincident PMT charge (ESUM) or possibly non-PMT detector subsystems such as the neutral current detectors (NCDs). The trigger system also triggers the detector at a regular rate (5 Hz in the current detector configuration), which has proved extremely useful for studying detector activity (e.g. PMT noise rates) in an unbiased way. The utility of this pulsed global trigger (PULSE_GT) in the trigger efficiency measurement is discussed in Section 6.3.

In addition to global trigger generation, the trigger also handles many other important system tasks. It provides a set of programmable calibration pulses for measurement of front-end charge/time pedestals and slopes. This is implemented using an on-board pulser and precision delay circuitry which is programmable through the data acquisition system (DAQ). The trigger system also provides a user interface to the detector for calibration sources by

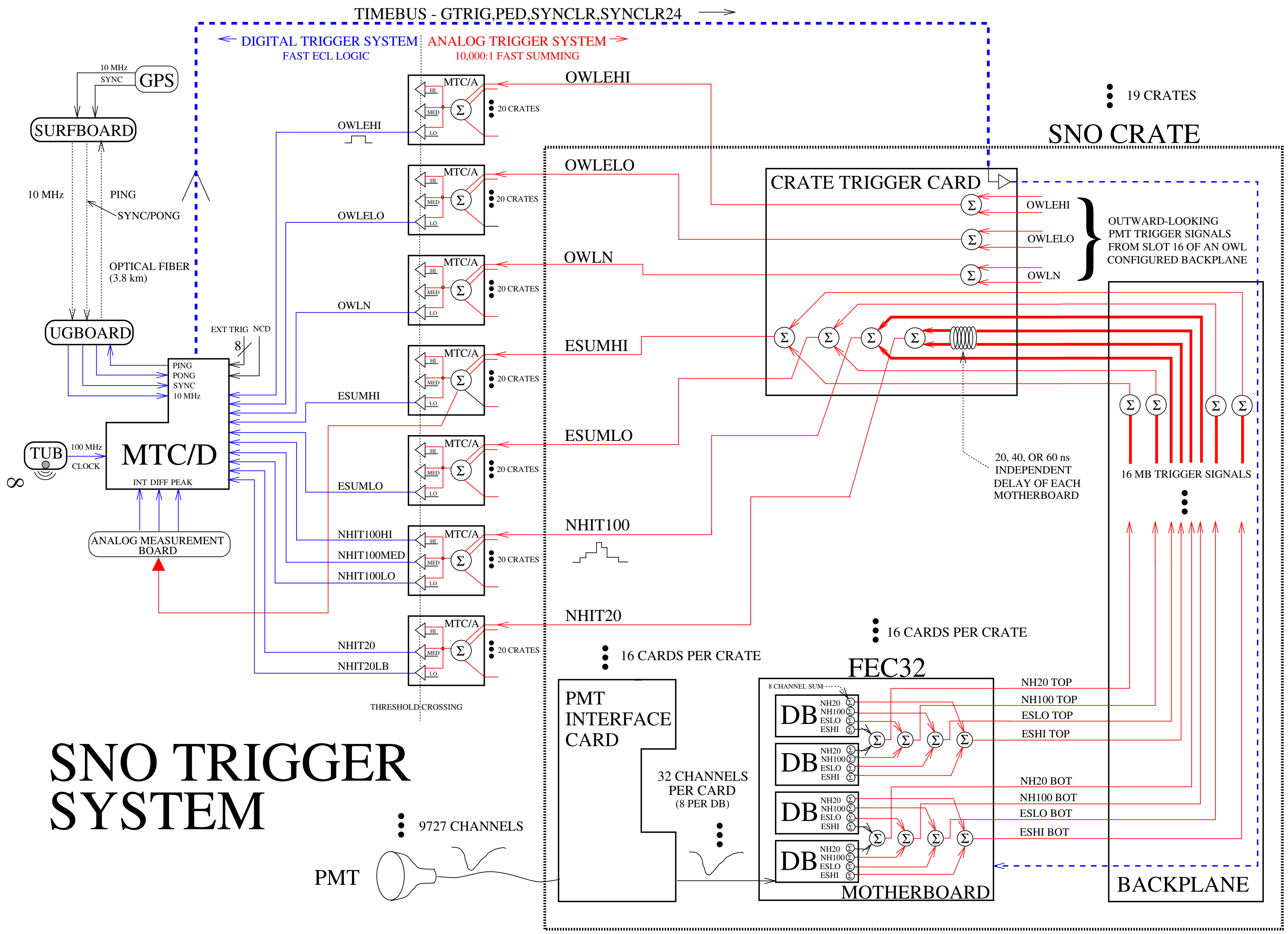

Figure 1: Block diagram of the the SNO trigger system

including a number of external trigger inputs as well as a utility board for analog pulse discrimination.

The trigger system is also responsible for maintaining and recording trigger-related event information such as inter-event timing, absolute event time, global trigger ID number, and information on which trigger types fired during an event. The inter-event timing is recorded by latching a 50 MHz counter that is sourced by a local 100 MHz ECL oscillator. Absolute time is maintained for correlating SNO events with astronomical observations by interfacing the system to a GPS receiver on the surface. This interfacing is handled by two fiber optic transceiver boards - one on surface and one underground - which transmit a 10 MHz GPS clock as well as a synchronization signal from the GPS receiver to the trigger system hardware over roughly 4 km of fiber. These interface boards also "ping-pong" the synchronization signal between surface and the detector underground to allow measurement and monitoring of the synchronization delay. In terms of global trigger identification, a 24-bit counter is latched and incremented on each event so that the count represents a unique event ID (up to roughly 16 million triggers) for a particular run. Each front-end channel also has a similar counter to allow association of PMT and trigger related data for building events, so the trigger system is also responsible for keeping these channel-level counters in synchronization with the central trigger counter. This is accomplished by sending a synchronization pulse to each channel on 16-bit rollovers of the central global trigger counter (i.e. every 65536 events), which sets an error flag on out-of-sync channels as well as synchronizes them to the central counter.

As depicted in Figure 1, the trigger system is naturally divided into analog and digital subsystems. The crossing of a channel-level discriminator threshold (e.g. in response to a PMT signal) initiates two equal amplitude current pulses of different duration - 20 ns and 100 ns - to enter independent analog summing networks. Shaped versions of the actual PMT signals are also separately summed, but while this energy-sum ("ESUM") trigger is extremely useful, it is not the main trigger for neutrino interactions nor is it relevant to the NHIT trigger efficiency and is not further discussed in this report (see [1] for more information). The trigger primitives of all channels in the system are summed together to form a final analog "NHIT" sum in the central trigger crate, however, in practice the final sum is current limited to about two crates worth of hits (1024 channels). This final sum is then fed into a current mirror which produces four identical copies of the analog sum. One copy is used for monitoring and the other three go to independent comparators for discrimination. Each comparator fires if its respective copy of the analog sum exceeds a threshold voltage set by a 12-bit digital-to-analog converter (DAC). Therefore, the analog system begins with the firing of channel-level analog trigger primitives that are subsequently summed together and ends with comparison of the final NHIT sum to three different DAQ-programmable thresholds for discrimination.

The front-end to the digital trigger system is the receiving of ECL trigger pulses on the inputs of the digital Master Trigger Card (MTC/D). These are sometimes referred to as "raw" trigger pulses, since they are candidate pulses for initiating a global trigger (i.e. generating an event in the detector). The output of the three comparators discriminating the 100 ns NHIT analog sum, called the N100LO, N100MED, and N100HI triggers, are examples of raw triggers that make up the "physics triggers" of the detector. While these three are the main physics triggers for the detector, others include the 20 ns NHIT thresholds, low and high gain ESUM triggers, and a set of outward-looking PMT triggers (see [1] for a complete description). There are also a number of external raw trigger inputs for calibration devices (e.g. laser, ^{16}N) and other systems requiring absolute time tagging (e.g. GPS synchronization signals, NCDs, hydrophone). In addition, there are a number trigger signals internal to the MTC/D that are treated in the same way as the external raw trigger signals in terms of their global trigger generation and latching. These include the PULSE_GT trigger already mentioned as well a PEDESTAL calibration trigger, a PRESCALE of the N100LO physics trigger, a DAQ-initiated "software trigger" (SOFT_GT), and a special trigger (SPECIAL_RAW) which fires on a programmable logical combination of nine pre-selected physics and external raw triggers. Table 2 contains a complete list of the 26 raw trigger types implemented in the SNO trigger system.

An understanding of the global trigger generation logic as well as the how the system stores information about which triggers fired in an event is necessary to understand how the trigger efficiency is measured. Figure 2 shows a schematic diagram of the trigger latching and global trigger generation logic involved in the digital trigger system. The way that the *digital* trigger system decides when to trigger the detector is actually quite simple. A set of 20 ns ECL raw trigger pulses (see Table 2) are input to the global trigger generation logic.

Mask bit	Raw trigger	GT?	Type	Raw trigger description
0	N100LO		External	Low threshold 100 ns
1	N100MED	$\surd$	External	Med threshold 100 ns
2	N100HI	$\surd$	External	High threshold 100 ns
3	N20	$\surd$	External	Normal 20 ns
4	N20LB		External	Low threshold 20 ns
5	ESUMLO		External	Low-gain energy sum
6	ESUMHI	$\surd$	External	High-gain energy sum
7	OWLN	$\surd$	External	Outward-looking PMT 100 ns
8	OWLELO		External	Outward-looking PMT low-gain energy sum
9	OWLEHI	$\surd$	External	Outward-looking PMT high-gain energy sum
10	PULSE_GT	$\surd$	Internal	Pulser generated
11	PRESCALE	$\surd$	Internal	Prescaled N100LO
12	PEDESTAL		Internal	Pedestal calibration
13	PONG	$\surd$	External	GPS synchronization delay
14	SYNC	$\surd$	External	GPS synchronization
15	EXT_ASYNC		External	External not synchronized to 50MHz clock
16..22	EXT2..8		External	External generic input
23	SPECIAL_RAW		Internal	Special logic programmable
24	NCD		External	Neutral-current detector input
25	SOFT_GT	$\surd$	Internal	DAQ-generated

Table 1: The 26 raw trigger types of the SNO trigger system. A global trigger resulting from any of these signals, except for the EXT_ASYNC external input, is synchronized to the 50 MHz system clock. A $\surd$ in the third column indicates the raw trigger types that are masked in for global trigger generation during production neutrino data taking. The type (external, internal) indicates whether the corresponding trigger is externally input to the MTC/D or is generated on the board (through the DAQ or otherwise).

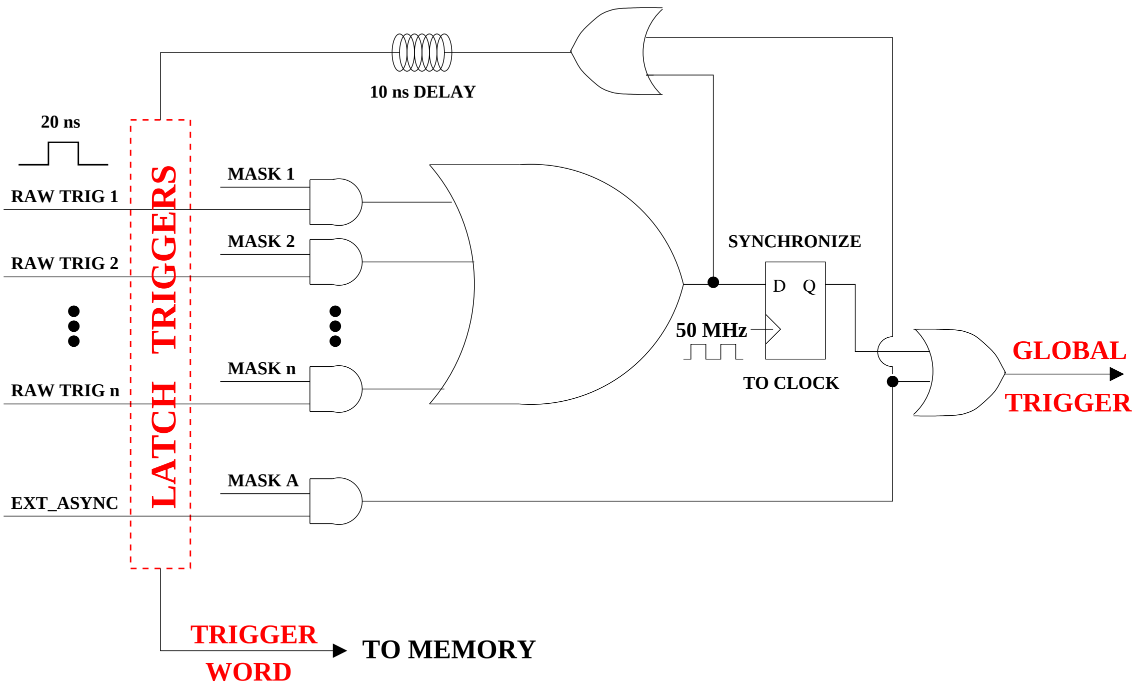

Figure 2: Schematic diagram of the trigger latching and global trigger generation logic involved in the digital trigger system. This is meant to depict logic flow and should not be interpreted as a literal schematic of discrete logic elements in the trigger electronics.

Each raw trigger encounters a DAQ-programmable mask bit that determines whether or not any signal from that trigger input will continue on to the rest of the generation logic. As such, only masked in raw trigger types are permitted to initiate events in the detector. The signals from all masked in *synchronous* triggers (i.e. all except EXT_ASYNC) are **OR**'d together and a valid output of this **OR** initiates a global trigger on the next tick of the 50 MHz clock. This synchronization of the global trigger to the system clock is important for maintaining robust digital operation of the MTC/D (for latching of counters, memory, etc.) and also leads to the so-called "20 ns jitter" of the PMT times event-to-event. It is important to note that since the front-end time measurement is operated as a common-stop system (i.e. each TAC ramp is started when the channel fires and stopped on a common global trigger[1]), this synchronization only jitters the overall time offset of each event relative to other events and *does not* smear the individual PMT times relative to each other (like the 1.6 ns jitter inherent to SNO PMTs) within an event.

It is, however, sometimes useful to sum up a large number of events and have the summed PMT time spectrum remain sharp, without smearing due to the global trigger synchronization. An example of such an application is laser PCA calibration of the PMT cable delays. Therefore, to accommodate these types of applications, an alternative trigger path (EXT_ASYNC) is provided for asynchronous global trigger generation (see Figure 2).

Aside from depicting the global trigger generation logic, Figure 2 also shows how information is stored about which triggers fired in a particular event. When one or more masked in raw trigger fires, the **OR** of these signals is not only synchronized to the system clock for global trigger generation but also acts as a latch of any valid raw triggers. This latch signal is delayed $\sim$ 10 ns (adjustable with an RC circuit) before sending a "snapshot" of the state of *all* raw triggers to the on-board memory for storage. This snapshot of the raw trigger inputs along with a "missed trigger" status bit (to be described later) make up what is referred to as the "trigger word" of the event. Note the important fact that on each event, the trigger system latches *all* 26 raw triggers, independent of their mask state and whether they are synchronous or asynchronous triggers.

The coincidence window for raw triggers to be latched together into the trigger word is determined by their pulse width and the latch delay, as well as their timing relative to the

[1]or when the channel resets itself after waiting a time GTVALID$\sim$ 390 ns without receiving a global trigger signal.

earliest masked in raw trigger which fires (i.e. the raw trigger that initiates the global trigger and determines the trigger timing). Figure 3 shows a diagram of the coincidence window involved in trigger word latching. Note that in an ideal sense, all raw triggers arriving within ± 10 ns of the earliest masked in raw trigger are latched into the trigger word, as well as the raw trigger that initiated the global trigger itself. In actuality, variations in the raw trigger pulse width as well as differences in signal propagation times to the latching logic slightly change the condition for coincident triggers at the point they are externally input to the MTC/D. This has implications for the trigger efficiency measurement using externally triggered calibration sources such as the laserball and will be addressed later. In addition to bits corresponding to the state of each raw trigger at latching time, the trigger word also contains a "missed trigger" status bit. This bit is set if any *masked in* raw trigger arrives after the latching time but before the end of the trigger cycle (~ 420 ns), as shown in Figure 3.

3 Trigger Efficiency and Acceptance

A measurement of the NHIT trigger efficiency involves answering the following question:

> For a given trigger hardware threshold, with what probability does the detector trigger as a function of the number of channels hit in coincidence?

In this context, two channels are considered "in coincidence" if they fire within the NHIT coincidence time of each other determined by the average width of the analog primitives summed together - 93 ns for the NHIT100 trigger and 20 ns for the NHIT20 trigger. The answer to this question is a curve for each hardware trigger threshold setting, which gives the trigger probability as a function of $\tilde{N}$, the number of coincident, or "in-time", hits. If the shape of the trigger efficiency curve is the same over all relevant threshold settings, then it may be sufficient to simply translate one measured curve rather than apply a different curve for each threshold, but this needs to investigated with calibration data. It is certainly important to measure the efficiency curve at the current trigger thresholds set in the production data taking. In addition, for higher energy analyses it may be sufficient to know at what NHIT (actually $\tilde{N}$) we are 100% efficient rather than the detailed shape of the trigger efficiency curve, as previously mentioned.

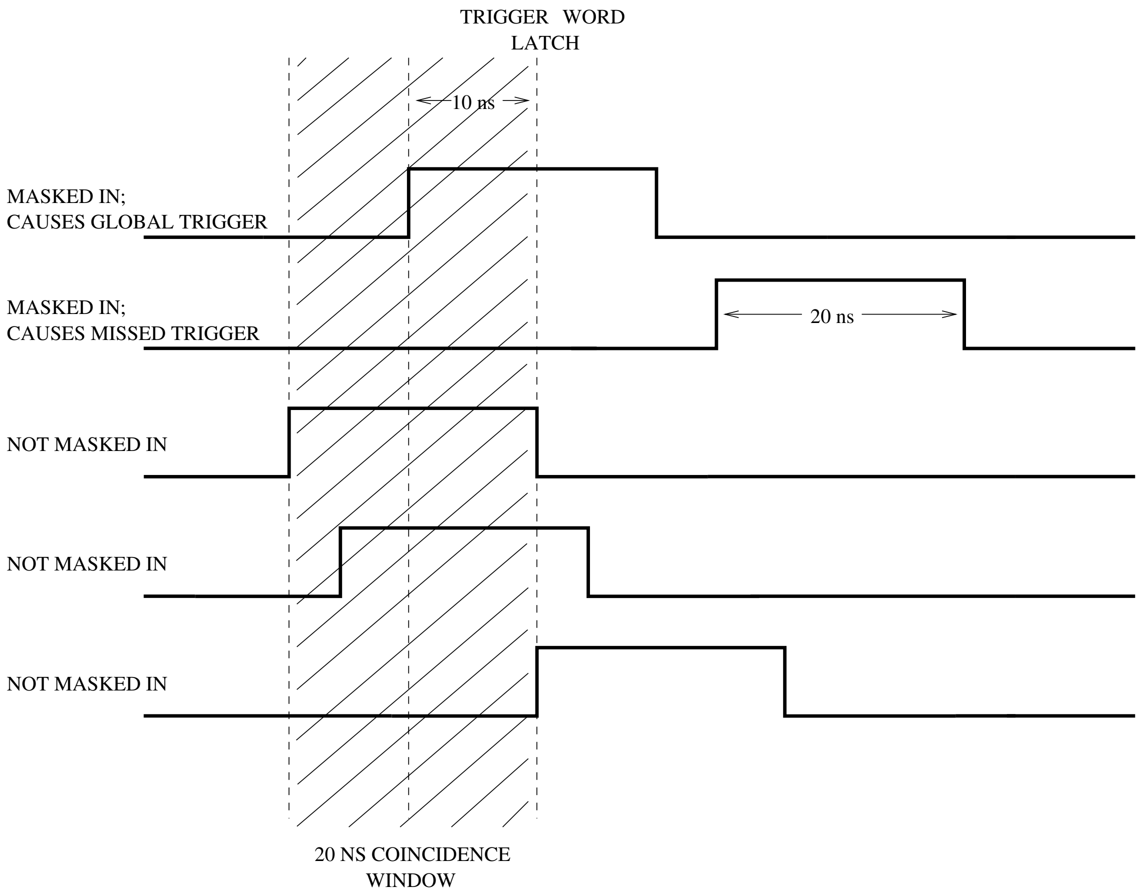

Figure 3: Diagram showing the coincidence window involved in trigger word latching. Each pulse represents a different raw trigger signal arriving at the global trigger generation logic. Note that raw triggers arriving within ± 10 ns of the raw trigger that initiates the global trigger are latched into the trigger word. Also shown is how a masked in raw trigger arriving after the latching time during the trigger cycle causes the "missed trigger" bit to be set in the trigger word.

It is important to distinguish between trigger efficiency and detector acceptance. The acceptance is the probability for the detector to trigger on a particular type of physics signal (e.g. a 5 MeV electron at (0,0,0) in the +z-direction). While the trigger efficiency depends solely on the performance of the detector hardware (and DAQ), the acceptance is much more difficult to determine and depends on many things, some of which are listed below:

- Trigger efficiency for the triggering conditions (trigger thresholds, masks)
- Optical properties (attenuation/scattering in H_2O/D_2O/AV, AV/PMT reflectivity)
- Detector gain (PMT gain/Q.E., channel efficiencies)
- Geometry (event position/direction, PMT geometry, etc.)
- Physics (Particle energy, Cerenkov light production, electron scattering, etc.)

Therefore, the trigger efficiency is an important piece of information for understanding our detector acceptance, but it is only one piece. Other calibration data and physics/detector simulation is needed to fully estimate the acceptance in the absence of absolute calibration sources.

4 Trigger Inefficiencies

Although at this point we have not presented any results on the measured trigger efficiency, we anticipate that, despite our best intentions, SNO does not have a perfectly efficient trigger. As such, we present in this section a few sources of inefficiencies that can lead to deviations from a perfect step-function trigger (see Figure 4).

As discussed in Section 2, the trigger system is largely an analog system. This has numerous advantages over a digital system, including speed (fast trigger determination leading to small trigger and channel dead time) and simplicity (trigger information contained in single analog sum). However, maintaining the analog integrity of an approximately 10^4 channel sum from 19 separate crates (each of which are bustling with digital activity) to a central rack over 100 ft of cable provides its own set challenges. Below are some analog characteristics which can lead to inefficiencies in the system:

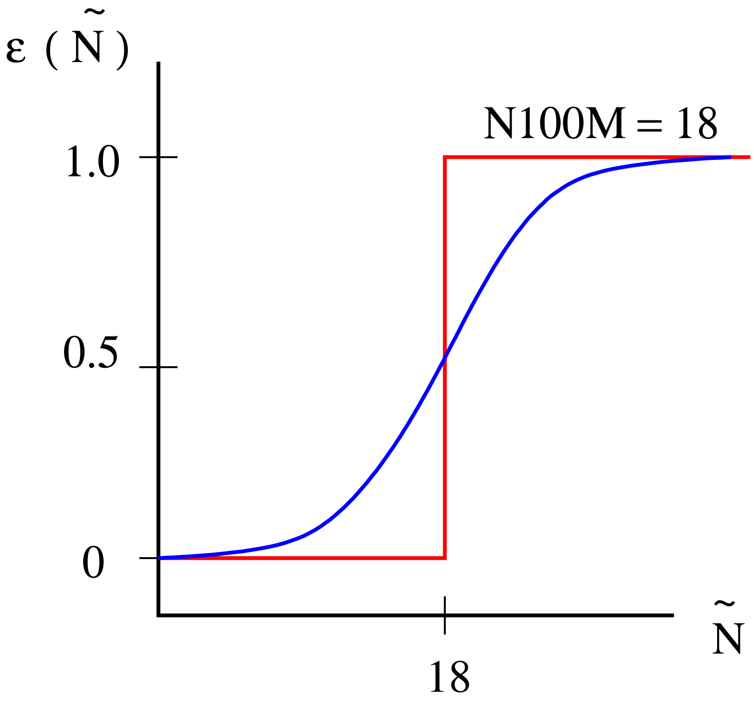

Figure 4: Dramatization of how the various sources of trigger inefficiencies can alter the trigger efficiency curve in an ideal system (shown in red, where $\tilde{N}$ is the number of in-time hits). The true trigger efficiency curve (in blue) may also be translated along the $\tilde{N}$-axis by some types of inefficiencies so that the 50% efficiency point is no longer where $\tilde{N}$ equals the hardware trigger threshold.

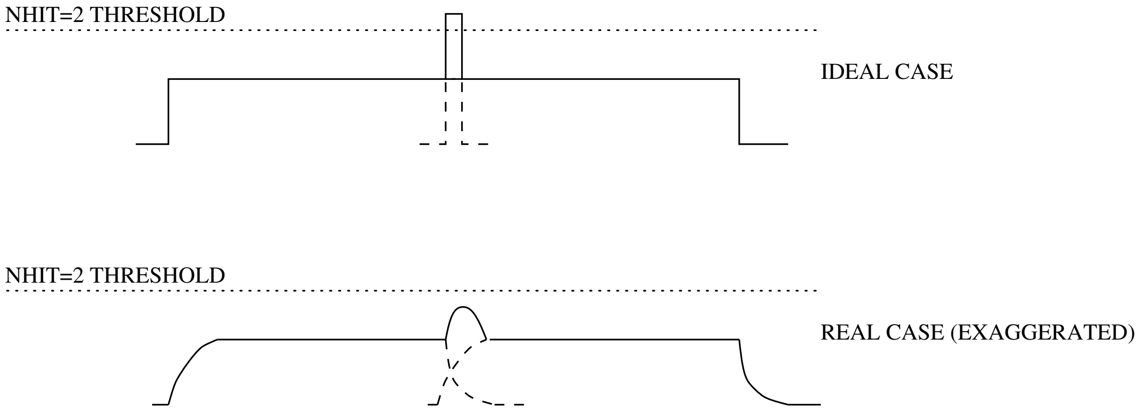

Figure 5: Exaggerated diagram of the effects of analog pulse shape on trigger efficiency. In the Figure, a threshold set at NHIT=2 triggers for ideal pulses, but not for those with finite rise and fall times.

- **Finite rise/fall of analog trigger primitives**: Much of the analog trigger design effort went into generating sharp analog trigger primitives and maintaining short rise/fall times throughout the entire NHIT sum. However, some degradation of the trigger pulses is inevitable (e.g. some integration by cable capacitances, etc.) and this results in a loss of efficiency (see Figure 5). This effect gets larger as the trigger pulses get more out of time, so we expect this type of inefficiency to be worse for events originating away from the center of the detector where geometric effects will spread out the PMT hit times.

- **Variations in width/amplitude**: Ideally, all analog trigger primitives are exactly the same - 30 mV in amplitude and either 20 ns or 93 ns in duration depending which trigger type we are talking about (NHIT20 or NHIT100) - regardless of which channel fires to give the pulse. In reality, there is a nonzero spread in the distribution of both width and amplitude of the analog primitives which leads to a smearing of the trigger efficiency curve.

- **Electronics noise/pickup**: Any type of electronic noise that is picked up on the trigger lines can lead to inefficiencies in the trigger by altering the shape of the analog sum. This can lead to spurious misses or extra global triggers, depending on the shape and sign of the pickup as well as where in the analog sum it occurs.

- **Baseline/threshold variations**: Any changes in the DC offset of the analog sum or the hardware threshold will change the effective NHIT threshold (unless, of course, both change by same amount and in the same direction) and lead to a smearing of the trigger efficiency. These changes could be due to some low frequency pickup, temperature variations, $1/f$ noise in the current mirror elements, etc.

Aside from these "features" of an analog system, there are some other important sources of trigger inefficiencies worth mentioning:

- **CMOS (a.k.a "NHIT") dropout**: This is actually a special type of baseline variation. In this case, the baseline shift is by one unit of NHIT and can last for milliseconds or longer, depending on the average rate of the offending channel causing the dropout. What happens is that occasionally a channel-level discriminator will fire in response to a very short threshold crossing in time (i.e. noise or the tip of a PMT signal) and signal the CMOS chip to fire with a runt signal rather than full pulse. These runt pulses can turn on the current source within a CMOS chip that is the NHIT=1 analog primitive but fail to turn it off. This current is then summed into the analog network (as is the current from all other channels) and results in a DC-like shift in the analog sum baseline for as long as the channel is "stuck". Fortunately, this current source seems to get "un-stuck" by the next normal firing of that channel, so the baseline shift from a single channel lasts on average only a few milliseconds ($\sim$ 500 Hz channel rates). However, the dropout is frequent enough so that with $\sim 10^4$ channels contributing, random dropout coincidences lead to a continually fluctuating baseline of $\sim 1 - 2$ NHIT in magnitude. Since the baseline shift due to a given channel always has the same sign - it always *lowers* the effective trigger threshold for a period of time - this causes the system to trigger at a lower number of in-time hits than it would otherwise and leads to a shifting of this efficiency curve toward lower $\tilde{N}$.

- **Orphans**: Since the number of in-time channels, $\tilde{N}$, is determined by counting hits in the event, any channels that fire and contribute to the NHIT sum but are dropped from the event data stream appear as a trigger inefficiency. These "orphan" PMT bundles are either associated into the wrong event (i.e. they have a GTID matching a trigger GTID still in the event builder's circular buffer) or are collected with other orphan PMT bundles into an "orphanage". These orphan PMT bundles can either be due to a corrupted GTID in a PMT data bundle (hardware orphans) or inefficiencies in the readout/building of events (software or readout-related orphans).

- **Digital inefficiencies**: It is also possible that digital inefficiencies can contribute to the shape of the trigger efficiency curve. For example, how often does a raw trigger pulse from a masked in trigger not generate a global trigger? For healthy raw trigger pulses (20 ns in duration with normal ECL logic levels), production testing of the digital boards with calibration pulses indicates that this contribution is negligible. However, similar to the case of CMOS dropout, discrimination of the final analog sum can lead to runt raw triggers from the MTC/A one-shot to be input on the MTC/D. In this case the MTC/D will still issue a global trigger, however the trigger word latch arrives after the end of the masked in runt raw trigger pulse initiating the event. Since the detector *does* trigger on this threshold crossing its not a loss of efficiency but rather a loss of information about which masked in raw trigger fired.

- **Dead trigger channels**: Channels which are active in acquiring data but do not contribute to the NHIT trigger sum are an obvious source of inefficiency. In some sense, these channels are exactly opposite to orphans which contribute to the NHIT analog sum but do not give any data to the event. These channels could be inactive because of a hardware problem (e.g. CMOS problem) or their signal path is broken in some way. Alternatively, these channels may have their triggers deliberately disabled due to some other trigger problem (e.g. excessive CMOS dropout), however there is trigger status information put in the data stream by the DAQ which allows one to know how many disabled channels contributed to a particular event.

5 Methods of Measurement

In order to measure the NHIT trigger efficiency, we need a source of correlated hits to determine the trigger system response to a variety of situations encountered in normal data taking. In the early days of system development, pedestals were used as such a source since we could fire any desired number of channels using the MTC/D on-board pulser. The problem with using pedestals, however, is that they are too in-time and do not provide a stringent enough test of the analog trigger system to feel comfortable about the system performance under the battle conditions of asynchronous data.

The laserball calibration source provides a triggered source of correlated light in the detector, leading to correlated PMT hits needed for the NHIT trigger efficiency measurement. The light from the source is approximately isotropic light with sharp timing (~ 2 ns) and the source can be moved around the detector to test the position dependence of the efficiency. Another important feature of the laserball system for trigger efficiency is the ability to vary the intensity of the light so that we can test the occupancy dependence and map out as much of the efficiency curve as possible.

It is also possible to use normal NHIT triggered data as a source of correlated hits to estimate the trigger efficiency. In this case, we use the fact that in normal data taking there are multiple thresholds on the same NHIT sum, so we can use the lower threshold as a triggered "source" of correlated hits to study the response of the higher NHIT threshold.

Eventually, it would be useful to check the trigger efficiency results with some combination of the ^{16}N and the pT calibration sources, which would allow a measurement using Compton scattered electrons rather than diffused laser light. There is no advantage in using this data over the laserball source data except as a redundant check and possibly the psychological advantage of using data more closely resembling the data upon which the trigger efficiency results will be applied (i.e. events due to Cerenkov light). The problem with only using ^{16}N calibration data is that it does not have sufficient coverage in NHIT to sample the interesting parts of the trigger efficiency curve (i.e. near threshold).

In this section, two approximate trigger efficiency measurement methods using the laserball calibration source and NHIT triggered data are presented along with their shortcomings. Then, the current best method for trigger efficiency determination using the laserball and more robust trigger latching technique is discussed in detail.

5.1 Approximate MTC/D Latch Methods

The methods discussed in this section all are approximate methods used as a check on the more robust method described in section 5.2. These methods all use bits in the MTC/D trigger word to determine which NHIT triggers fired in an event. As discussed in Section 2, the latching of these bits requires close timing between the NHIT raw triggers and the particular masked in trigger initiating the global trigger. This type of narrow latching is desirable for determining coincident triggers during normal data taking, but can lead to phantom inefficiencies in our trigger efficiency measurements. The reason for this is simple - just because a particular trigger misses getting latched into the trigger word does not mean that it *by itself* as a masked in trigger would not have generated a global trigger. As an example, imagine that we are analyzing NHIT triggered data with N100MED = 18 and N100HI = 20 trigger thresholds masked in (actually, its only necessary that N100MED is masked in for this example). An event originating at the center occurs with 18 prompt hits perfectly in-time that fire the N100MED trigger and 3 hits due to (PSUP) reflections with come ~ 70 ns later. Even if the N100HI raw trigger fired, it would not get latched into the trigger word since it comes much later than the trigger word latch so we would say there were 21 hits in 93 ns coincidence and the N100HI missed. However, if the N100HI raw trigger *did* fire and it was the only trigger masked in, then we would have triggered the detector on this event. Clearly this sort of situation will lead to an underestimation of the trigger efficiency. Even in the absence of reflection triggers, a difficulty with using this method of determining which triggers firing in an event is knowing exactly how to count the number hits, $\tilde{N}$, that contribute to an NHIT trigger firing which could get latched into the trigger word along with the raw trigger that initiated the event. The MTC/D latch methods also get more difficult as the source is moved away from the center of the detector, since it becomes even more difficult to maintain the close timing between the triggers necessary for their coincident latching.

5.1.1 Laserball with MTC/D Latch

This method uses laserball light as a source of correlated hits and the MTC/D trigger word to determine which triggers fired in each event (see Figure 6). Each laser pulse is coupled through a set of fiber optic cables to a diffusing ball (the laserball) in the detector to produce an approximately isotropic source of light with adjustable intensity. There is also a PIN diode monitoring the light from the laser which supplies a trigger for the diffused light in the detector. This PIN diode signal is discriminated by a pulser which provides an

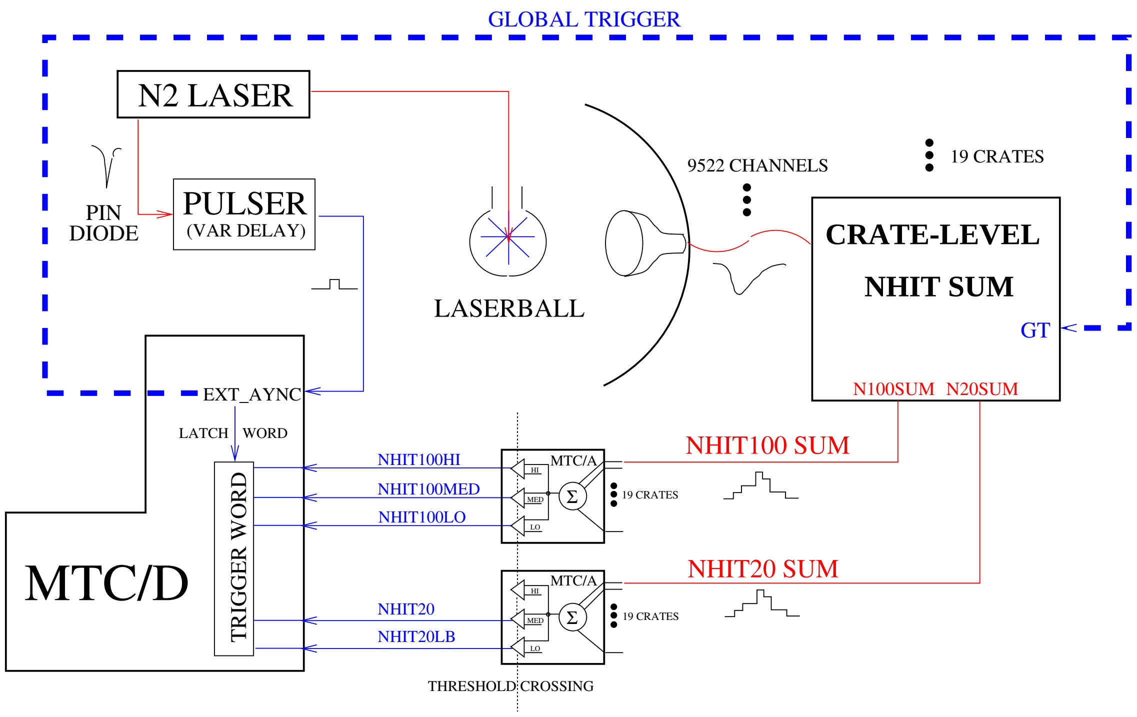

Figure 6: Block diagram of trigger efficiency measurement method using the laserball with MTC/D trigger word as the trigger latch.

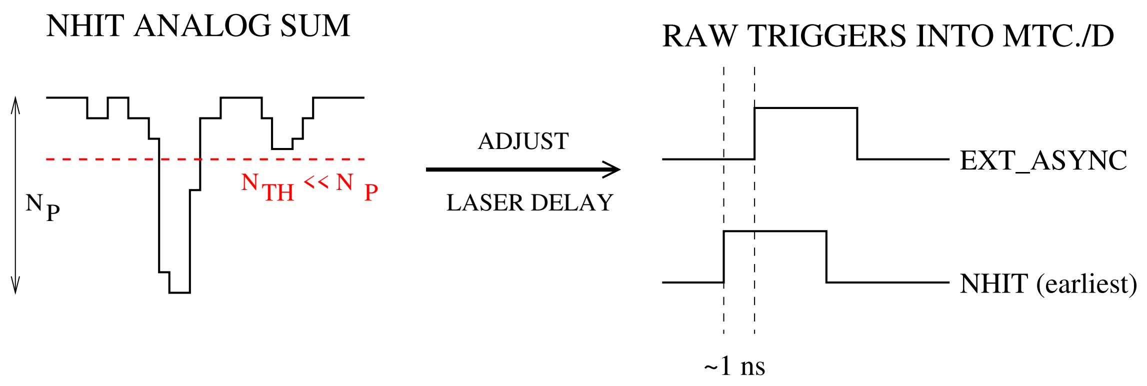

Figure 7: Laser trigger timing for the trigger efficiency measurement using the MTC/D latch method. The NHIT threshold, N_{TH}, is set so that it is small compared to the number of prompt hits, N_P, from the laser light. The laser delay is then adjusted until the majority of the early NHIT raw triggers are slightly (1 ns or so) earlier than the laser raw trigger pulse at the EXT_ASYNC input on the MTC/D.

adjustable delay between the PIN diode pulse and a 20 ns ECL pulse that is sent to an external (asynchronous) trigger input on the MTC/D. A global trigger (GT) is then issued by the MTC/D since we mask in the EXT_ASYNC trigger type, and all other triggers firing $\sim$ 10 ns before or after this external trigger are latched into the trigger word (recall Figure 3). The actual latch timing is slightly modified from this when the measured raw trigger widths are included, which is discussed later in this section.

In order to latch a large fraction of the NHIT triggers firing on the laser light, careful adjustment of the pulser delay controlling the laser trigger timing is required. This is done by setting the NHIT trigger threshold to be small compared to the number of prompt hits from the laser light, and then adjusting the pulser delay so that the laser trigger arrives at the MTC/D one ns or so *later* than the majority of the *early* NHIT raw triggers (see Figure 7). The timing is done this way partly because of walk effects on the trigger - at a given threshold, the trigger will fire later as the amplitude (i.e. NHIT) approaches threshold. In addition, differences in PMT cable lengths (and, to a lesser degree, trigger signal trace/cable delays) as well as channel-level discriminator walk effects contribute to the spreading out of the NHIT trigger timing. Therefore, we adjust the laser trigger delay, which determines the trigger latch timing, to cover the largest possible range of NHIT trigger firing times on the prompt laser light.

In order to determine the trigger efficiency curve at a given threshold, a static window is applied to the PMT time spectrum for each event to count the number of in-time hits, $\tilde{N}$, in the event. In this context, "static" means that the size and position of the window applied to the hit times is the same for each event because the laser trigger is *not* synchronized to the system clock and hence there is no common stop time jitter. Whether or not the NHIT trigger fired on a particular number of in-time hits is determined by the trigger word - only if the NHIT trigger in question was latched into the MTC/D trigger word is it considered to have fired in the event. As previously mentioned, this method of determining if the NHIT trigger fires in an event is too restrictive due to the small latching window, so we expect this method to underestimate the trigger efficiency near threshold. For a given value of $\tilde{N}$, the trigger efficiency is the ratio of the number times the NHIT trigger is observed to fire to the total number $\tilde{N}$ occurrences over all events. Different $\tilde{N}$ parts of the trigger efficiency curve are sampled by variations in the laser intensity from fluctuations at a given intensity or by purposely changing the amount of light with neutral density filters.

To get the value of $\tilde{N}$ for each event, we would like to construct a PMT time window to count the number of in-time channels contributing to the analog sum such that a raw trigger firing in response to the sum can get latched into the trigger word along with the laser trigger (EXT_ASYNC). The size and position of this static time window is determined in the following way. As described in Section 2, all raw triggers arriving within 10 ns of the masked in trigger that causes the global trigger are latched into the trigger word. However, this assumes a raw trigger width of 20 ns which is not quite true in reality. A measurement of the raw trigger pulse width for the NHIT triggers indicates that they are actually closer to 26 ns, so the latching window is slightly modified. In general, for a latching delay δ_{latch} and NHIT raw trigger width δ_{pulse}, the NHIT trigger will get latched into the trigger word with EXT_ASYNC (which is the only masked in trigger type and initiates the global trigger) if it arrives within a time interval

$$[t_{laser} - \delta_{pulse} + \delta_{latch}, t_{laser} + \delta_{latch}]$$

where t_{laser} is the arrival time at the global trigger generation logic of the EXT_ASYNC trigger (see Figure 8(a)). Therefore, we want to construct our static window on the PMT

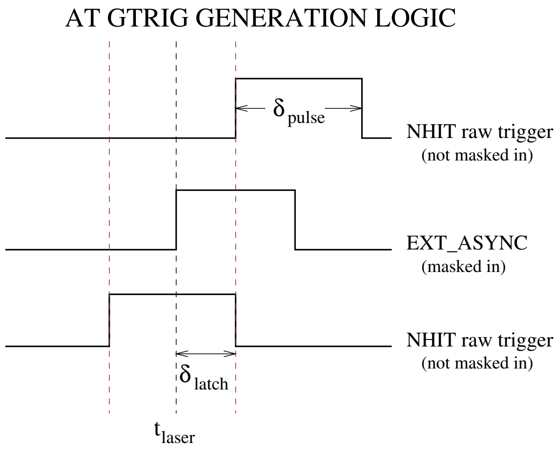

(a)

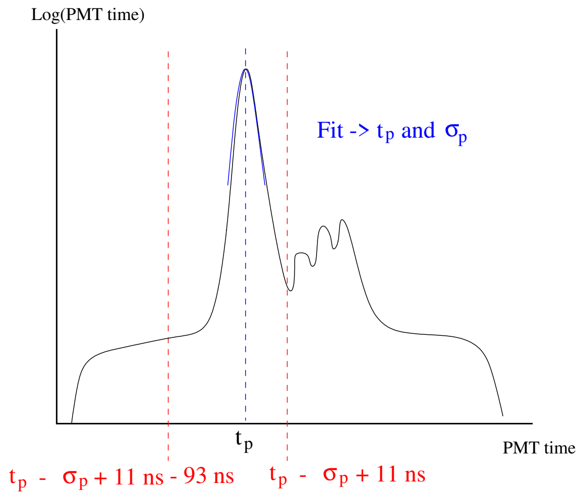

(b)

Figure 8: (a) Diagram showing the general latching case between a masked in raw trigger (EXT_ASYNC) and another raw trigger which is not masked in (NHIT). (b) Picture showing how the window used to count the number of in-time channels is determined from the summed PMT time spectrum.

times so that if the NHIT trigger fires on the analog sum produced by the channels in the window, its timing is such that the raw trigger produced can be latched into the trigger word (i.e. is within the latching coincidence interval). While the width of the time window is determined by δ_{pulse} and δ_{latch}, the absolute position offset seems unconstrained because of the unknown delays of the system (both the NHIT trigger path as well as laser trigger). However, we did determine this offset position by adjusting the laser delay so that the onset of the NHIT trigger firings at a low trigger threshold due to the laser light arrived at the MTC/D ~ 1 ns before the EXT_ASYNC pulse from the laser trigger (recall Figure 7). We use this fact to relate t_{laser} to the PMT hit times in the event by assuming that the onset of the NHIT trigger firings at low threshold occurred at a PMT time 1σ earlier than prompt peak. Therefore, we fit prompt peak in the summed PMT time spectrum over many laser events to a Gaussian and relate t_{laser} to t_{prompt} and σ_{prompt}, the mean and standard deviation of the fit, respectively, by

$$t_{laser} = (t_{prompt} - \sigma_{prompt}) + 1 \text{ ns}$$

Substituting this into the relation for the latching interval with $\delta_{pulse} = 26$ ns, $\delta_{latch} = 10$ ns, and $\sigma_{prompt} \sim 2$ ns (see Table 2 in Section 6.1.1) gives

$$[t_{prompt} - 17 \text{ ns}, \, t_{prompt} + 9 \text{ ns} \,]$$

One final modification to the interval is made - since the NHIT100 trigger primitives are all ~ 93 ns in length, channels contribute to analog sum over that the time period after firing so we extend the front edge of the interval to match this width. The final window interval is then

$$[t_{prompt} + 9 \text{ ns} - 93 \text{ ns}, \, t_{prompt} + 9 \text{ ns} \,]$$

which gives the 93 ns coincidence window used determine $\tilde{N}$ for each event. Figure 8(b) shows a picture of how the window used to count the number of in-time channels is determined from the summed PMT time spectrum.

To summarize the method described in the section, a window is applied to the PMT time spectrum of each externally triggered laser event to determine $\tilde{N}$ by counting the number of hits in this window. In this context, $\tilde{N}$ is the number of in-time channels contributing to the analog sum such that a raw trigger firing in response to the sum can get latched into the trigger word along with the laser trigger (EXT_ASYNC). For each $\tilde{N}$ occurrence, the trigger efficiency is the ratio of the number of times the particular NHIT trigger fired - determined by whether or not the corresponding bit was set in the trigger word of that event - to the total number of $\tilde{N}$ occurrences.

Although there was some attempt at a rigorous determination of the proper time window for this method of measurement, the truth of the matter is that the uncertainty in the size/position of the window applied to the PMT times is probably a reasonable fraction of the actual raw trigger coincidence window size. This is dominated by a lack of exact knowledge on how the observed timing between the EXT_ASYNC and the onset of the NHIT raw trigger firings relates to the absolute window position in the PMT time window. In addition, this method is awkward for investigating the source position dependence of the trigger efficiency since the prompt peak is distorted for sources off-center implying that the raw trigger timing needs to be recalibrated at each position. For these reasons, this method is considered an approximate check on the results of the method presented in Section 5.2, which uses a more robust latching method to determine whether or not a particular NHIT trigger fired in an event.

5.1.2 NHIT triggered data

This method is similar to the laser method described in the previous section, except that normal NHIT triggered events are used as the source of correlated hits rather than events from diffused laser light. It may seem circular to estimate the NHIT trigger efficiency in this way, however, the fact that we are able to independently trigger on multiple thresholds of the same NHIT analog sum allows us to estimate the trigger efficiency with this type of data. This method still has all the same problems with correctly determining if a particular NHIT trigger actually fired in the event inherent to using the MTC/D trigger word at the latch. In fact, things may be worse with this method in terms of latch timing because NHIT triggered data involves sources of light distributed throughout the detector in all different directions.

The way the method works is that two different thresholds on the NHIT trigger sum are set and the lower threshold trigger is masked in to generate global triggers. The resulting events are analyzed in the much the same way as the laser data, except now the lower NHIT trigger threshold acts as a trigger for the light rather than the PIN diode pulse. Another important difference in using normal NHIT data is that there is no explicit determination of the raw trigger timing as in the laser setup, so we do not know exactly where in the spectrum of PMT times to place our in-time channel window. What we do in this case is estimate the lower threshold crossing time by "discriminating" an ideal trigger sum constructed from the PMT times and apply a sliding window around this time. This type window positioning needs to be done separately for each event since the shape of the trigger sum varies between events and also because of the 20 ns jitter of PMT times caused by synchronization of the global trigger to the 50 MHz clock (see Section 2). Figure 9 depicts how the sliding window used to count the number of in-time channels, $\tilde{N}$, is constructed from the PMT time spectrum of NHIT triggered event.

Determining the trigger efficiency using NHIT triggered data and the methods described in this section is more difficult than the laser method described in Section 5.1.1. There is a certain degree approximation that goes into determining the proper latch window and some potential systematic bias in assuming a perfectly efficient trigger in constructing the analog sum from the PMT times. Specifically, it is difficult to know exactly when the lower threshold raw trigger fires to initiate the event, so the proper position of the latching window is estimated using an analog sum constructed from the PMT times. It may be possible to better guess the latching window with a more realistic trigger simulation that includes measured properties of analog trigger primitives (i.e. rise/fall time, amplitude, superimposed noise, etc.) or by using information about the phase of the global trigger synchronization[2]. Clearly, additional work needs to be done here to make a more accurate measurement of the trigger efficiency using NHIT data. Therefore, the results of the current method - as well as the laser MTC/D latch method of Section 5.1.1 - should be considered an approximate check on the method described in the next section. However, using the production neutrino data to estimate the NHIT trigger efficiency is potentially very useful since it allows one to track changes in the efficiency over time without having to setup and perform the laser measurement each time.

[2]As of 12/16/99, the *unsynchronized* global trigger signal has been connected to channel 21 of the FEC/D for event-by-event tagging of the synchronization time offset.

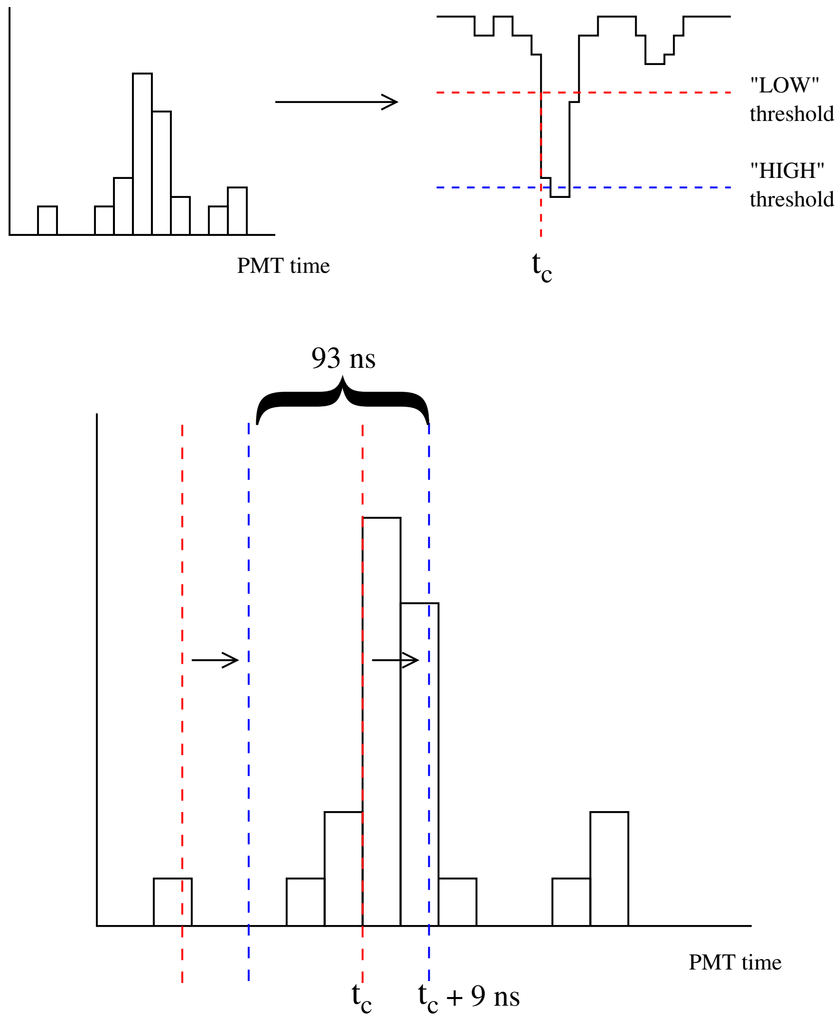

Figure 9: Description of the in-time channel window used in estimating the trigger efficiency from NHIT triggered data. (top) From the hit PMT times in an event, an ideal analog sum is generated assuming equal amplitude 93 ns trigger primitives with zero rise and fall time. The threshold crossing time, t_c, is determined from the time at which the ideal sum exceeds the lower hardware NHIT threshold. (bottom) A 93 ns sliding window is placed around t_c to count the maximum number of in-time channels, $\tilde{N}$, within the coincident raw trigger latching region for this event. The back edge of the 93 ns sliding window is varied from t_c to $t_c + 9ns$ and number of hits in each window position counted to determine the maximum number, $\tilde{N}$.

5.2 Laserball with FEC/D Latch Method

To overcome the shortcomings of methods using the MTC/D trigger word as a latch of the NHIT triggers that fire in each event, a new method was devised which greatly increases the width of the latching window from 20 ns to $\sim$ 85 ns. This allows for a more realistic determination of which NHIT triggers fire along with the laser trigger (EXT_ASYNC) in a given event since we are much less sensitive to phantom inefficiencies resulting from narrow raw trigger timing (e.g. reflection triggers). In addition, the more robust trigger latching provides a natural way to measure the trigger efficiency for sources away from the center of the detector without having to change the laser trigger delay timing at each position.

The main idea of the method is to use the FEC/D channels - spare calibration channels in slot 15 of crate 17 - as the trigger word instead of the MTC/D. A block diagram of the system configuration during this method of measurement is shown in Figure 10. In the FEC/D laserball method, one or more of the NHIT raw trigger cables (i.e. the digital ECL lines after the discrimination of analog sum, see Section 2) feeding the MTC/D are disconnected. These lines are terminated and converted from ECL to TTL logic levels using one of the many useful features of the Trigger Utility Board (TUB[3]). These TTL lines are then connected to inverting transformers (i.e. transformers with their output lines switched - essentially an analog inverter) and each are plugged into one of the FEC/D channel inputs. So each of the FEC/D channels connected in this way receives a negative going TTL pulse when the corresponding NHIT trigger fires in an event.

The laser PIN diode provides a trigger for the diffused light in same way as described in Section 5.1.1, however the pulser delay timing is slightly different. In this method, the laser trigger is delayed as much as possible without losing prompt tubes off early side (the "curl") of the TAC window[4]. This moves the FEC/D channel times as early as possible to get the largest dynamic range on the NHIT trigger firing time. This dynamic range is constrained by the cable length to the FEC/D as well as how much the global trigger (initiated by the laser trigger) can by delayed without losing the earliest prompt light PMTs. With the laser trigger delays used for the measurements in this report, the dynamic range turns out to be $\sim$ 85 ns on the late end of the time the NHIT raw triggers fire the FEC/D channels on the

[3]sometimes also referred to as the Totally Useful Board.

[4]Note that *delaying* the laser trigger moves the tubes hit by light as well the FEC/D channels *earlier*.

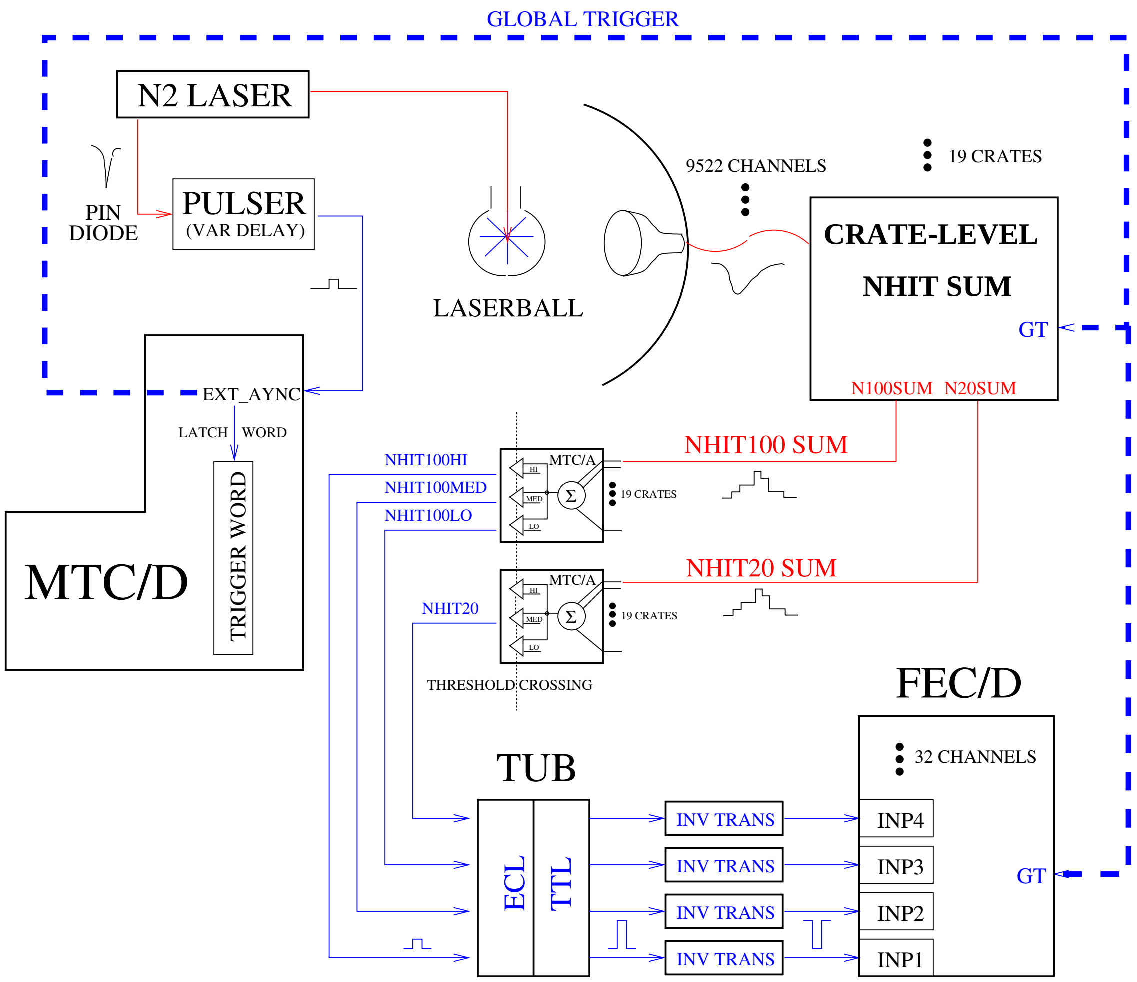

Figure 10: Block diagram of trigger efficiency measurement method using the laserball with the FEC/D as the trigger latch. The method is similar to the laserball MTC/D latch method discussed in Section 5.1.1, except now the hit status of the FEC/D channels determine which NHIT triggers fire during a laser event rather than bits in the MTC/D trigger word.

prompt laser light.

In terms of data analysis, we no longer constrain the window position applied to the PMT time spectrum since we have substantially increased the latching coincidence interval. Instead, a sliding 93 ns window is applied throughout entire spectrum of hit PMT times to determine the maximum number of in-time channels, $\tilde{N}$, in each event. To determine whether or not a particular NHIT trigger fired in a given laser triggered event, we simply look to see if the corresponding FEC/D channel is in the event. In practice, there is an additional check on the low gain integrated charge (QLX) for any FEC/D channel in the event to ensure that the channel fired on a TTL pulse from the corresponding raw trigger rather some sort of noise or pickup. Therefore, for a given value of $\tilde{N}$ representing the maximum number of hits in any 93 ns time window, the trigger efficiency is the ratio of the number times the NHIT trigger is observed to fire based on the FEC/D channels to the total number $\tilde{N}$ occurrences over all events.

6 Data Analysis and Results

In this section, the results of analyzing laserball and NHIT data using the methods described in Section 5 are presented. In addition, the consistency of the results from the laserball FEC/D latch method of Section 5.2 with the inferred rates from pulsed global trigger (PULSE_GT) data is discussed.

In this report, trigger efficiency results from the laserball methods are based on an analysis of laser calibration data taken on 10/25/99 and 10/26/99. The results of Sections 6.1.2 and 6.3 are based on NHIT and PULSE_GT events extracted from the production neutrino data (runs 10000 and greater). Full ECA/PCA calibration of the PMT times are applied in all analyses using standard ECA calibration constants from SNODB and PCA calibration constants derived from runs taken on 10/27/99. In regard to PMT timing calibration, it should be noted that only events with all hit PMTs passing the full timing calibration are considered in this analysis. This should not introduce any significant bias into the trigger efficiency measurement, but does reduce the amount of data usable for the analysis. In future analyses, it may be worth while reverting to ECA timing calibrations for events that fail the PCA calibration once this machinery exists. The reduction of data from failed PMT timing

Run #	Date taken	Avg NHIT	# of events	μ_{prompt} (ns)	σ_{prompt} (ns)
5735	10/25/99	19	74370	192.0	1.997
5736	10/25/99	10	73559	191.7	2.161
5738	10/25/99	65	81358	192.4	1.820
5760	10/26/99	17	24503	191.7	2.124
5761	10/26/99	60	25367	192.4	1.850
5762	10/26/99	7	27303	191.7	2.254

Table 2: Summary of trigger efficiency laser runs using MTC/D latch method. All laserball runs were at the center with a 40 Hz trigger rate. The parameters μ_{prompt} and σ_{prompt} are from a Gaussian fit to the prompt peak of the summed PMT time distribution for each run.

calibration is partly addressed in Section 6.1.1.

6.1 Approximate MTC/D Latch Methods

In this section, trigger efficiency results using the approximate methods described in Sections 5.1.1 and 5.1.2 are presented. Recall that these methods use bits in the MTC/D trigger word to determine which triggers fire during an event and subsequently arrive at the efficiency for a particular NHIT trigger. While these MTC/D latch methods involve some uncertainty in how to properly window the PMT times to get the number of in-time channels in each event, they provide important checks of the results from Section 6.2 which uses a more robust method of raw trigger latching.

6.1.1 Laserball with MTC/D Latch

The trigger efficiency laserball runs taken using the MTC/D as the trigger latch are summarized in Table 2. The different runs provide a range of laser intensities that cover several NHIT (and $\tilde{N}$) regions of the trigger efficiency curve. All runs were taken at a 40 Hz EXT_ASYNC trigger rate with the laserball very near the center of the detector.

Recall that the method described in Section 5.1.1 involves counting the number of hits in the time window

$$[t_{prompt} + 9 \text{ ns} - 93 \text{ ns}, t_{prompt} + 9 \text{ ns}]$$

to determine the number of in-time channels, $\tilde{N}$, for each event. The value of t_{prompt} is the prompt peak position from a Gaussian fit to the summed PMT time distribution. See Figure 11(a) for an example of the PMT timing distribution over all events in trigger efficiency run 5735. The Gaussian fit results for all runs relevant to this section are shown in the last two columns of Table 2 and the average values over these runs are $\overline{\mu_{prompt}} = 192.0$ ns and $\overline{\sigma_{prompt}} = 2.034$ ns. For simplicity, the we use $\overline{\mu_{prompt}}$ as the value of t_{prompt} for each run which yields the static window [108 ns, 201 ns] that is applied to the PMT time spectrum of each event to determine $\tilde{N}$. The trigger efficiency for a given $\tilde{N}$ and NHIT100 threshold is then the ratio of the number of times the trigger is observed to fire based on the MTC/D trigger word to the total number of $\tilde{N}$ occurrences.

As previously mentioned, failed timing calibrations can cause problems for the analysis because we need to know the time that each channel in the event fires to determine $\tilde{N}$. For all analyses in this report, events which fail the full ECA/PCA timing calibration are simply ignored. This should not lead to any significant bias in the trigger efficiency measurement unless failed channels have systematically different trigger characteristics than the rest of the channel population. It does, however, reduce the amount of usable data for the analysis, especially for higher NHIT data since probability of getting one or more failed calibration channel increases with the NHIT of the event. In future analyses, some data may be recovered by reverting to ECA only calibration for events where the PCA calibration fails, but one would have to verify that such a calibration scheme does not introduce any significant bias or noise into the measurement. As an example of failed calibrations involved in a typical trigger efficiency run, Figure 11(b) shows a distribution of the number of channels failing the full ECA/PCA timing calibration for events in run 5735. The full data reduction and NHIT distribution over all trigger efficiency runs listed in Table 2 is shown in Figure 12.

The measured trigger efficiency using the laserball with MTC/D latch method is shown in Figure 13 for the three NHIT trigger thresholds currently used in production data taking. According to the results from this method, the trigger turn-on (i.e. number of NHIT between 10% and 90% efficiency) is ~ 3.8 NHIT for each of the three thresholds and we are 100% efficient with our main physics trigger (N100MED = 18) for the detector somewhere between 23 and 24 NHIT (actually $\tilde{N}$, the in-time NHIT). Also, the shapes of the efficiency curves are quite similar, with the hardware threshold near 50% efficiency.

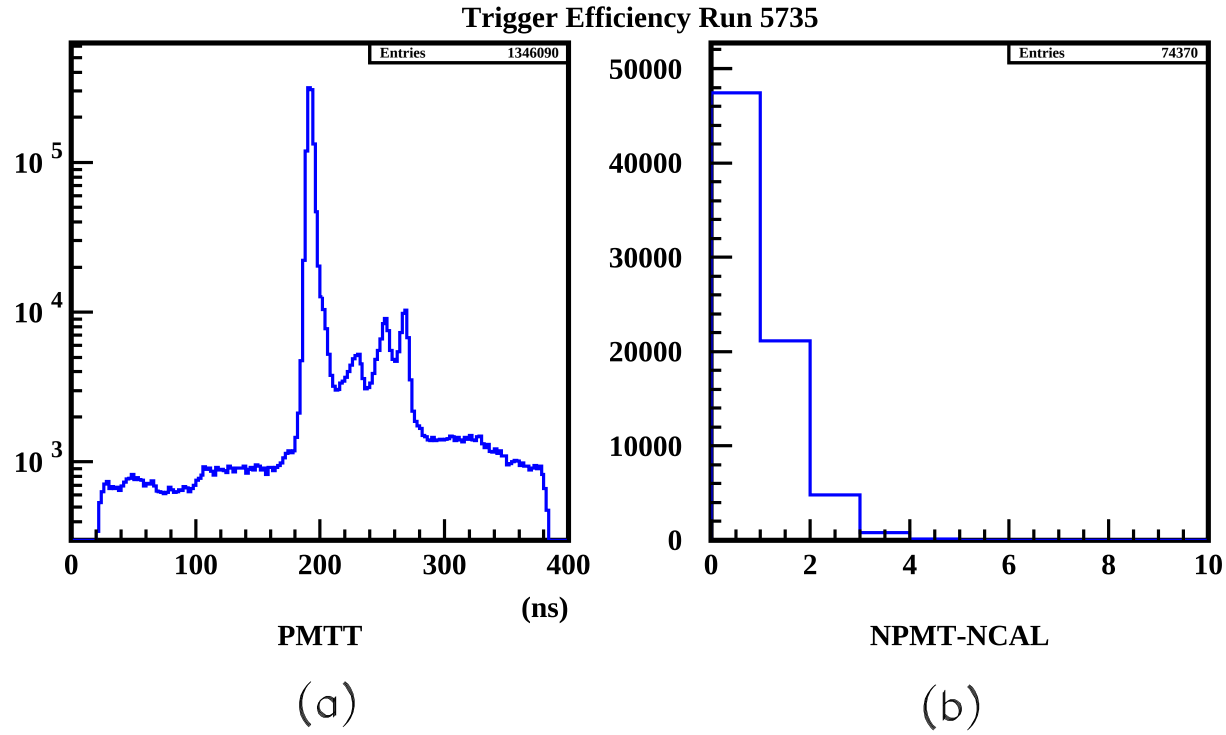

Figure 11: (a) Summed PMT time distribution for trigger efficiency run 5735. (b) Distribution of the number of channels failing the full ECA/PCA timing calibration for events in run 5735. The average occupancy of this run is approximately 19 NHIT and roughly 2.5% of the channels hit in this run failed the full ECA + PCA timing calibration. This gives an expected fraction of events with all channels passing the calibration of $\sim (0.975)^{19} = 62\%$ which is consistent with the fraction of events in the first bin of the figure.

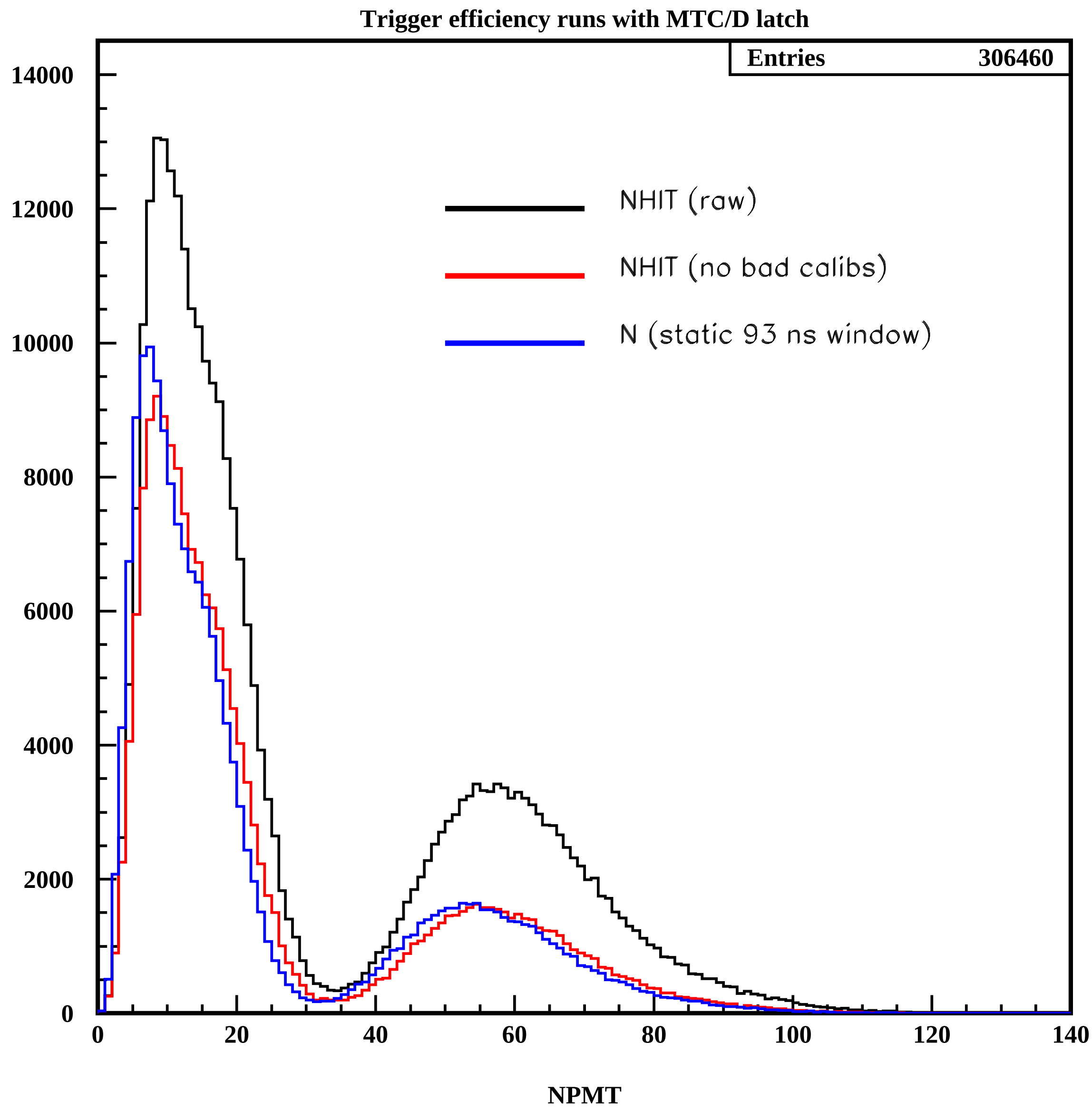

Figure 12: NHIT distribution of all events (black) and events having all hits passing the full ECA/PCA timing calibration (red) for the MTC/D latch method runs. Also shown (blue) is the distribution of $\tilde{N}$, the number of hits in a static 93 ns time window around the prompt light peak.

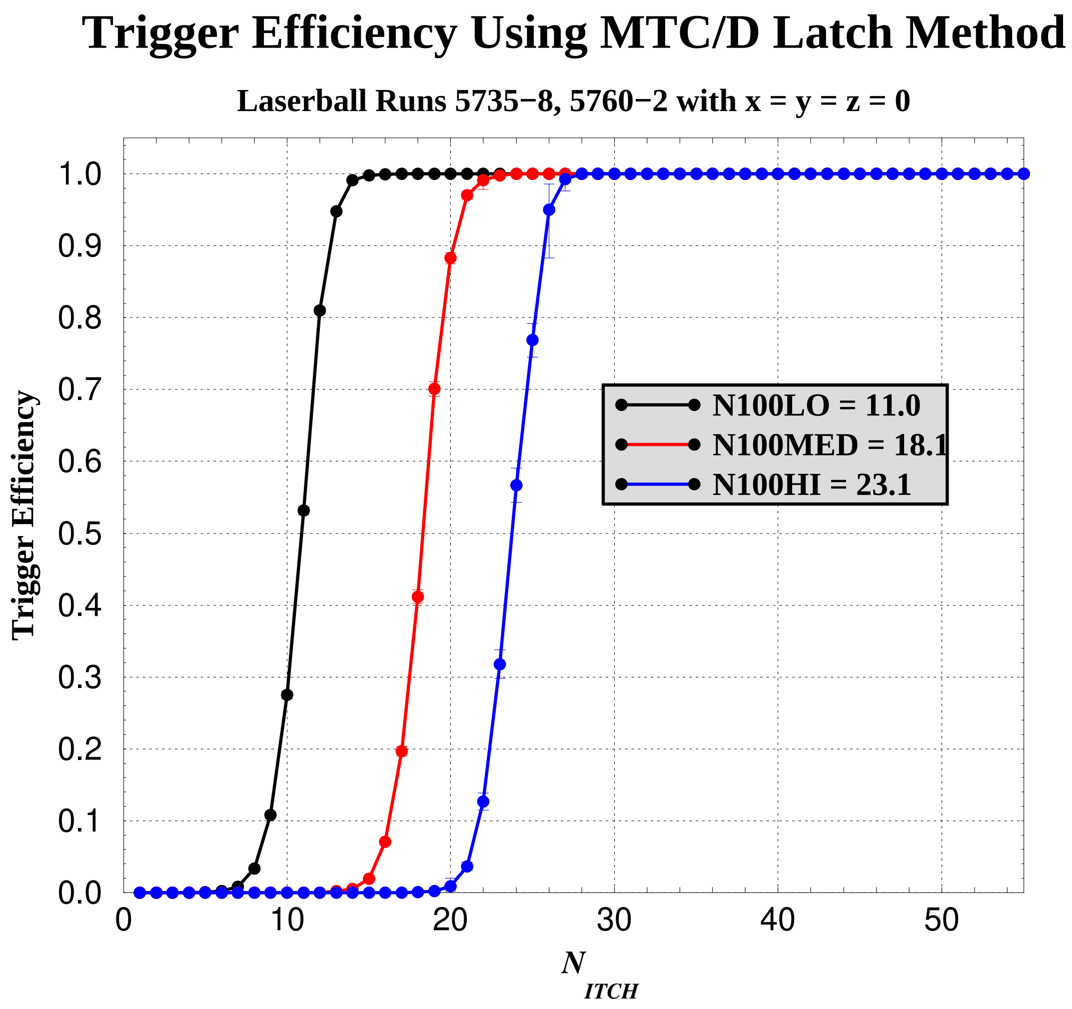

Figure 13: Measured trigger efficiency using the laserball with the MTC/D as the trigger latch. The laserball position is $x = y = z = 0$.

6.1.2 NHIT triggered data

In this section, trigger efficiency results using NHIT triggered events from the production neutrino data are presented. The analysis method was detailed in Section 5.1.2 where it was mentioned that in determining the proper position of the in-time channel window used to get $\tilde{N}$, some approximations are made regarding the shape of the analog trigger sum based on the PMT hit times and its relation to lower NHIT threshold crossing time. As such, the results of this method in its current form should be considered a rough check of other results.

The bulk of the data set used in the analysis was run 10237, which was a 59 hour neutrino run collected from 11/26/99 to 11/29/99. In order to get enough statistics at an NHIT above the bulk of the N100MED = 18 triggered events, the analysis also includes NHIT trigger events with $30 \geq NHIT \geq 50$ skimmed out of selected neutrino runs between 10000 and 10236. This provides a limited check on the important high efficiency region of the trigger efficiency curve.

In terms of data selection, only events with the N100MED bit set in the trigger word and no failed timing calibrations were included in the analysis. In addition, events where the MTC/D trigger word indicates that another *masked in* trigger - aside from the N100HI trigger which is the threshold being measured by this method - fired in coincidence with the N100MED are rejected. This includes ESUMHI, NHIT20, PULSE_GT, SYNC, PONG, and PRESCALE triggers (recall Table 2). The reason is because it is important for proper estimation of the latch window used to count the number of in-time channels, $\tilde{N}$, that the lower NHIT threshold (N100MED) firing determines the trigger timing rather than another trigger. The efficiency of the N100HI trigger (at a threshold of 23 NHIT) is then measured from these selected N100MED triggered events by counting for each event the maximum number of hits, $\tilde{N}$, a sliding 93 ns window (see Figure 9) and determining, based on the MTC/D trigger word, how often the N100HI trigger fires for a given $\tilde{N}$.

The trigger efficiency results are shown in Figure 14. Note that the statistics are still poor above $\tilde{N} = 30$, so one needs to augment the data sample with more high NHIT data if a better limit is desired. However, the shape of the curve is reasonably consistent with the N100HI threshold results using the laser with MTC/D latch method presented in Section 6.1.1, with a trigger turn-on of $\sim$ 3.8 NHIT and a similar 100% efficiency value of $\tilde{N}$ ($\sim$ 28). There is a slight shift by $\sim$ 0.5 NHIT between the two curves which may be due to systematic

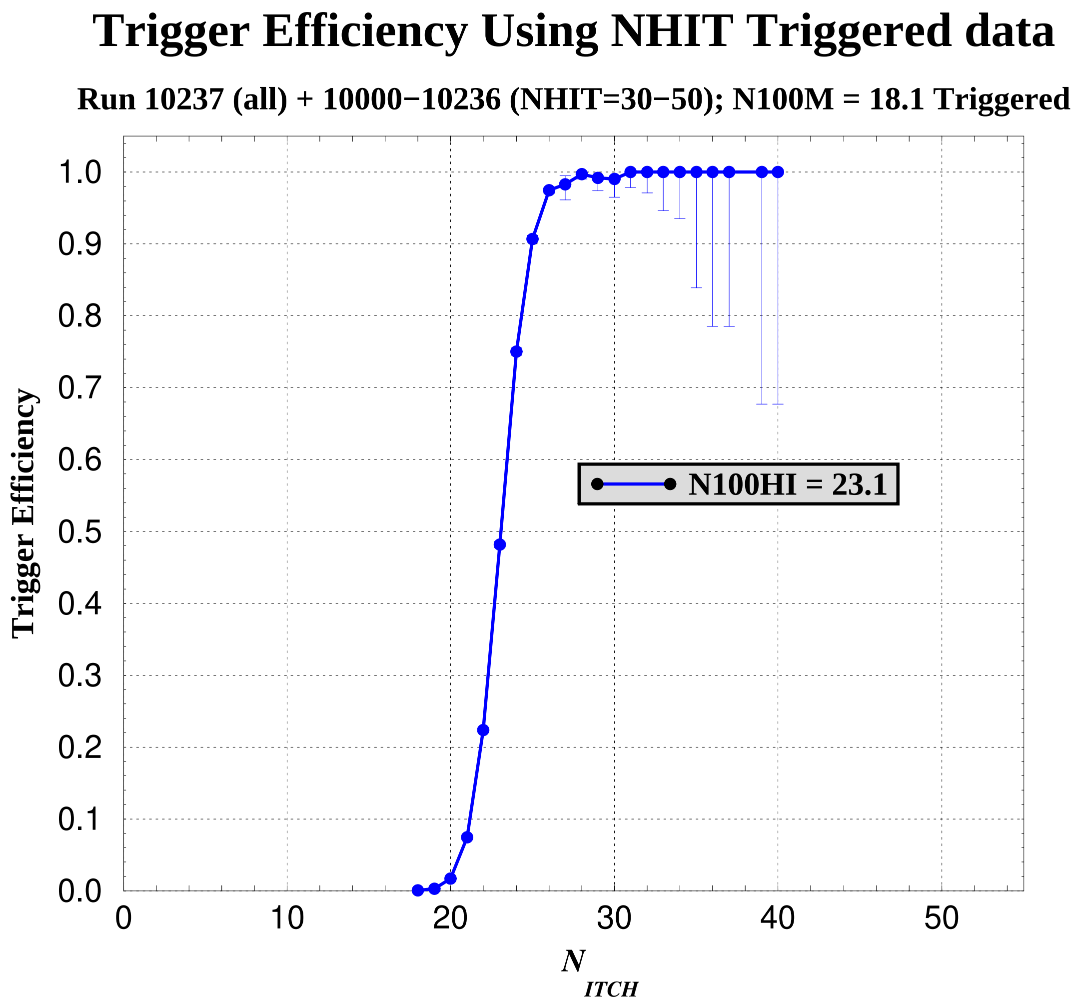

Figure 14: Measured trigger efficiency using the NHIT triggered data from standard neutrino runs.

differences between the methods (e.g. NHIT data samples all types of hit channel timing which differs from the analog sum profile for a laserball source at the center) or could be due to some slight change in the effective threshold between the runs (e.g. degree of CMOS dropout) since they were separated in time by a month. There also appears to be some structure near $\tilde{N} = 30$ beyond statistics which is not understood.

6.2 Laserball with FEC/D Latch Method

In this section, the results of the current best method for measuring the NHIT trigger efficiency are presented. As mentioned in Section 5.2 where the method is presented, this approach is similar to the laser with MTC/D method except it involves a much more robust way of latching of the triggers that fire in each event using special FEC channels rather than the MTC/D trigger word. This effectively increases the latching window from 20 ns to ~ 85 ns and removes the need for precariously positioned latching windows used to determine $\tilde{N}$, the number of in-time hits in an event. Instead, we now simply slide a 93 ns window throughout the PMT time spectrum to get $\tilde{N}$ and determine if a particular trigger fired by looking for the corresponding FEC/D in an event (and at the charge to ensure it fired on a TTL raw trigger pulse).

The trigger efficiency laserball runs taken using the FEC/D as the trigger latch are summarized in Table 3. The laserball source was run at the center of the detector as well as at z = -5 m (x = y = 0) to investigate the position dependence of the efficiency. Each source position data set is further subdivided into runs where N100MED and N100HI triggers were measured and runs were N100LO and N20 were measured. Measuring only two triggers once was simply due to available cable constraints at the time the data was taken - the actual number of triggers that can be measured in one run with the existing hardware using the FEC/D method is four, limited by the number of ECL$\rightarrow$TTL translators available on the TUB[5]. Table 3 shows an additional complication in the data taking - while N100HI and N20 were connected to the same FEC/D channel (ch 17) throughout, the N100LO and N100MED were connected to channel 6 for the runs on 10/25 but on 10/26 they were attached to channel

[5]The reason we do not simply run cables carrying the ECL signal to the FEC/D is that true ECL logic requires 50Ω termination to -2 V which the TUB supplies. The FEC/D input is AC coupling with 50Ω termination to GND.

Run #	Date taken	FEC/D channel				Laserball z(m)	Avg NHIT	Laser delay(ns)	LOCKOUT on TUB?	# of events
		100L	100M	100H	20					
5743	10/25/99	-	6	17	-	0	63	407	x	73361
5744	10/25/99	-	6	17	-	0	29	407	x	73571
5745	10/25/99	-	6	17	-	0	29	422	x	73200
5746	10/25/99	-	6	17	-	0	29	422		24684
5747	10/25/99	-	6	17	-	0	9	422		36742
5749	10/25/99	6	-	-	17	0	9	422		38507
5750	10/25/99	6	-	-	17	0	29	422		40720
5751	10/25/99	6	-	-	17	0	50	422		12334
5769	10/26/99	-	4	17	-	-5	18	422		73367
5770	10/26/99	-	4	17	-	-5	8	422		36706
5771	10/26/99	-	4	17	-	-5	54	422		42044
5773	10/26/99	4	-	-	17	-5	16	422		51497
5774	10/26/99	4	-	-	17	-5	51	422		56413
5775	10/26/99	4	-	-	17	-5	10	422		24559

Table 3: Summary of trigger efficiency laser runs using FEC/D latch method.

4. This was due to operator error and has no impact on the measurement except a slight annoyance in bookkeeping which FEC/D channels to look for in the analysis.

Also shown in Table 3 is the laser delay for each run, which determines the timing of the EXT_ASYNC trigger relative to the diffused light into the detector. Recall from Section 5.2 that in order to maximize the FEC/D latching window, we delay the laser trigger as much as possible without losing early tubes firing in response to the laser light. This is shown explicitly in Figure 15 which contains the raw TAC spectrum for events in runs 5743 and 5744 where the laser delay was increased from 407 ns to 422 ns, respectively. The sense of TAC is that the ADC counts are proportional to the time difference between the channel firing and the global trigger signal arriving at the channel so that early hits are toward the right of the spectrum and late hits to the left of Figure 15. Note that delaying the laser trigger by 15 ns moves the hit times *earlier* by $\sim$ 130 counts (by the shift in the prompt peak) which gives a rough overall calibration of 8.6 ADC counts / nsec. This yields an dynamic range for FEC/D latching of the raw triggers of approximately 85 ns on the late side of the prompt NHIT trigger firings[6]. For a given laser trigger delay, the position of the FEC/D prompt peak is determined by the standard delays in the trigger system as well as the cable delay of the raw trigger signal from the timing rack to FEC/D input in crate 17. Its possible that a more tailored cable length could gain some dynamic range here, but probably only a few ns. However, a more aggressive laser delay could push the FEC/D prompt peak maybe 40 or 50 ns earlier without significant loss of early inward-looking tube hits into the TAC curl region.

The range in occupancy as well as $\tilde{N}$ covered by the laserball FEC/D latch method trigger efficiency runs are shown Figures 16 and 17, for laserball source position at the center and at z = -5 m, respectively. Note the reduction in analyzable data due to bad calibrations as well as how the majority of hits are in-time (i.e. within the 93 ns trigger coincidence time of each other) at both source positions. The fact that most of the hits are "in-time" is of course because we picked our in-time window to match the width of the analog primitives that determine the trigger coincidence time which, by design, is long enough to include most hits. So there is nothing deep here, it just means that by parameterizing the trigger efficiency in

[6]We also have $\sim$ 280 ns on the early side of the prompt FEC/D peak, but any structure in that region would probably suggest a problem with pickup (e.g. from the laser) and thus not be used. No early structure of FEC/D hits is seen in any of the runs.

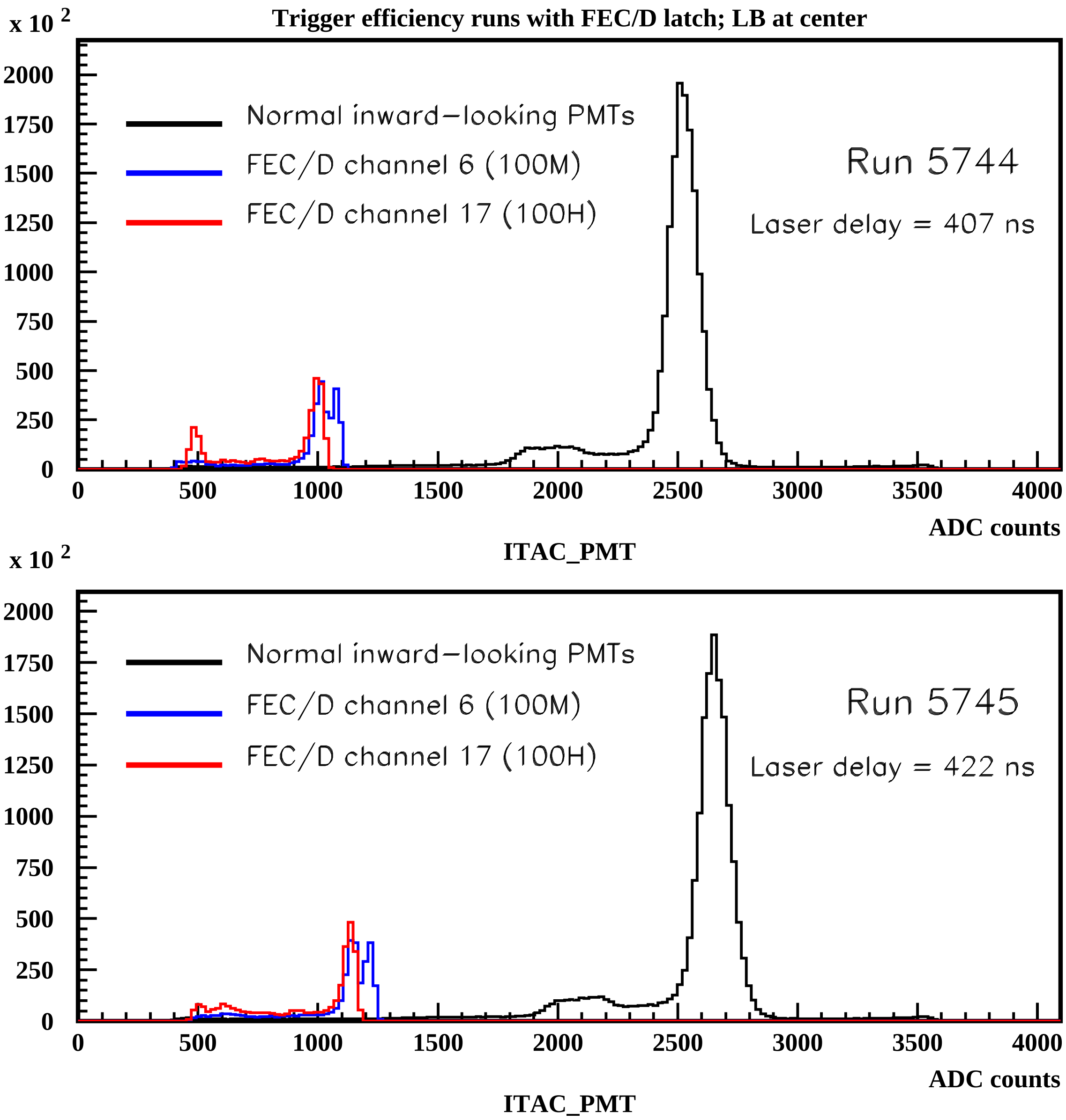

Figure 15: Uncalibrated TAC ADC counts for events from a laserball run at the center (top) and at z = -5 m (bottom).

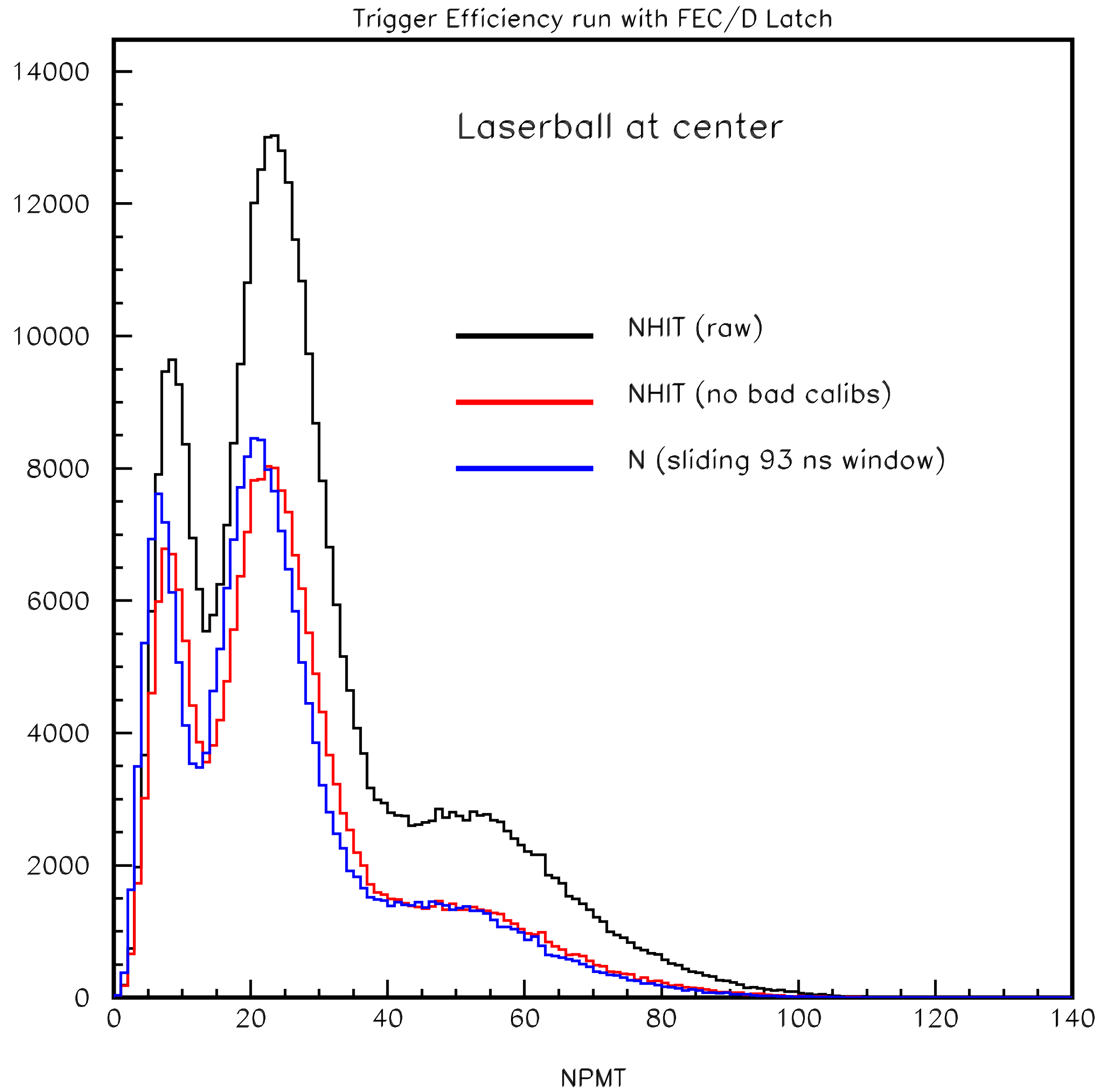

Figure 16: NHIT distribution of all events (black) and events having all hits passing the full ECA/PCA timing calibration (red) for the FEC/D latch method runs at the center of the detector. Also shown (blue) is the distribution of $\tilde{N}$, the number of hits in a static 93 ns time window around the prompt light peak.

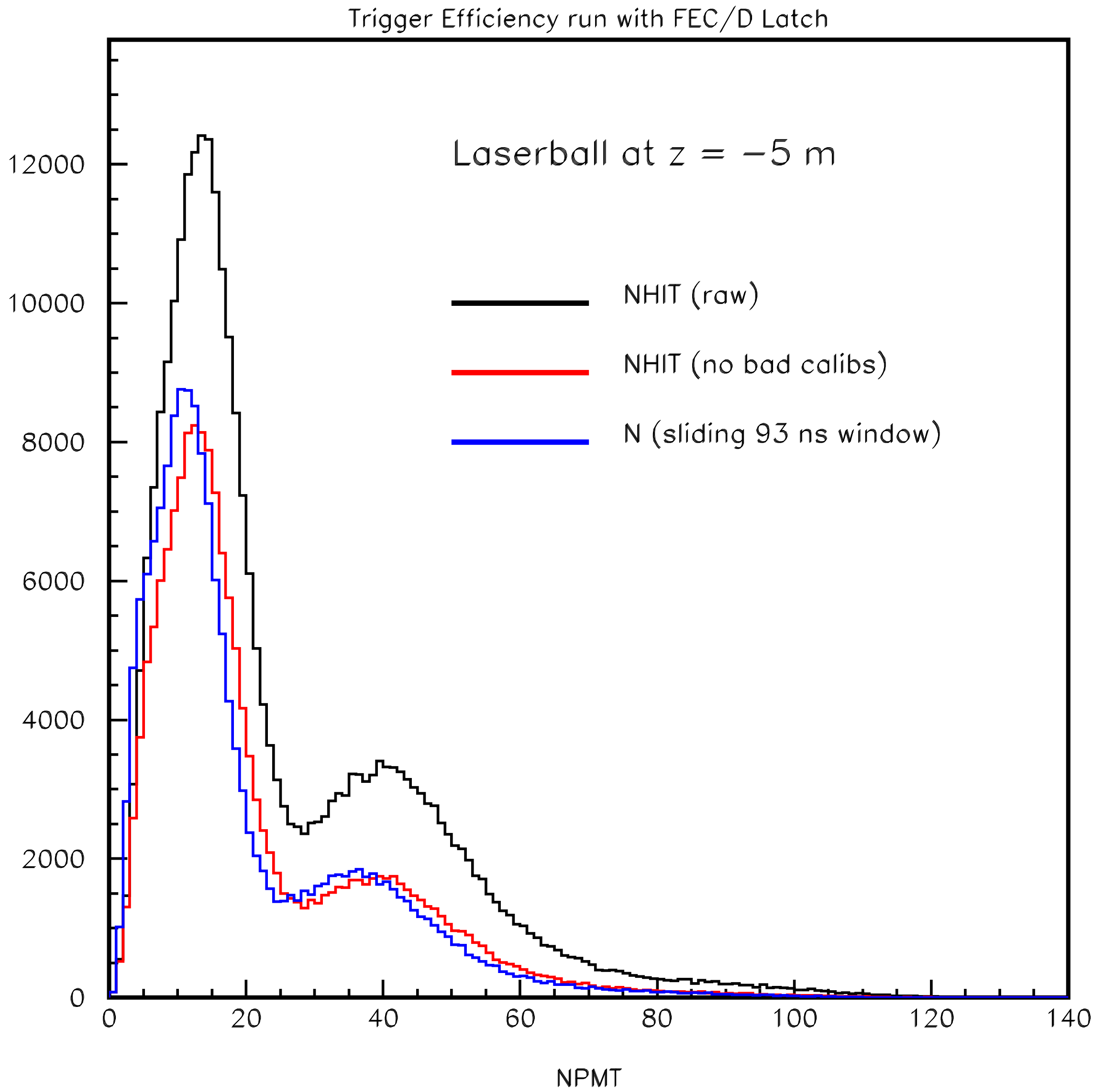

Figure 17: NHIT distribution of all events (black) and events having all hits passing the full ECA/PCA timing calibration (red) for the FEC/D latch method runs at z = -5 m. Also shown (blue) is the distribution of $\tilde{N}$, the number of hits in a static 93 ns time window around the prompt light peak.

this way, we get a close match between the NHIT of the event and $\tilde{N}$, with deviations due to reflections, scattering, PMT noise, etc.

In order to determine which (if any) of the measured triggers fired in a given laser trigger, we look to see which of the FEC/D channels connected to the raw triggers fired in the event. In addition, a charge cut is placed on any connected FEC/D channel in the event to ensure that only hits due to TTL-level raw trigger pulses are counted toward the trigger efficiency. Figures 18 and 19 show pedestal subtracted QLX plots for all FEC/D channels in events from laserball runs at the center and at z = -5 m, respectively. Note that for the channels connected to raw triggers (ch 4/6 and 17), the QLX measurement is quite unambiguous in that either the charge is near pedestal or very large. This means that determining when a FEC/D channel fires in response to a TTL raw trigger pulse as opposed to pickup is not a problem. Specifically, this determination is made by only accepting FEC/D channels with $QLX > 1250$. Note that in the FEC/D ch 4/6 and 17 charge distributions, there are some hits near pedestal which are probably due to crosstalk between these channels on the FEC/D. Recall that we are putting 5 V pulses into these front-end channels designed for PMT pulses of a few mV so there is likely to be some small amount of pickup, even with the FEC/D channel thresholds at maximum. The QLX distributions for FEC/D channels 4/6 and 17 all show a small amount of pickup, except channel 17 during the runs at the center (Figure 18) which shows a large spike near pedestal. This is yet another "feature" of the data taking, which is due to pickup on the TUB from a LOCKOUT TTL line routed right next to the $ECL \rightarrow TTL$ translation output. The LOCKOUT signal was disconnected after the first three runs (see Table 3) and this pickup spike disappeared from all QLX distributions after the disconnection.

To summarize the analysis method, we slide a 93 ns window around the entire PMT time spectrum for each event to determine $\tilde{N}$, the maximum number of hits within 93 ns of each other. The trigger efficiency of a measured trigger threshold is the ratio of the number of times that threshold fired for a given $\tilde{N}$ to the total number of $\tilde{N}$ occurrences. Whether or not a particular threshold fires in a given event is determined by the QLX charge of the corresponding FEC/D channel ($QLX > 1250$) if it fired during the event.

The results of the trigger efficiency analysis using the laserball with FEC/latch method are shown in Figures 20 and 21 for the laserball at the center of the detector and at z =

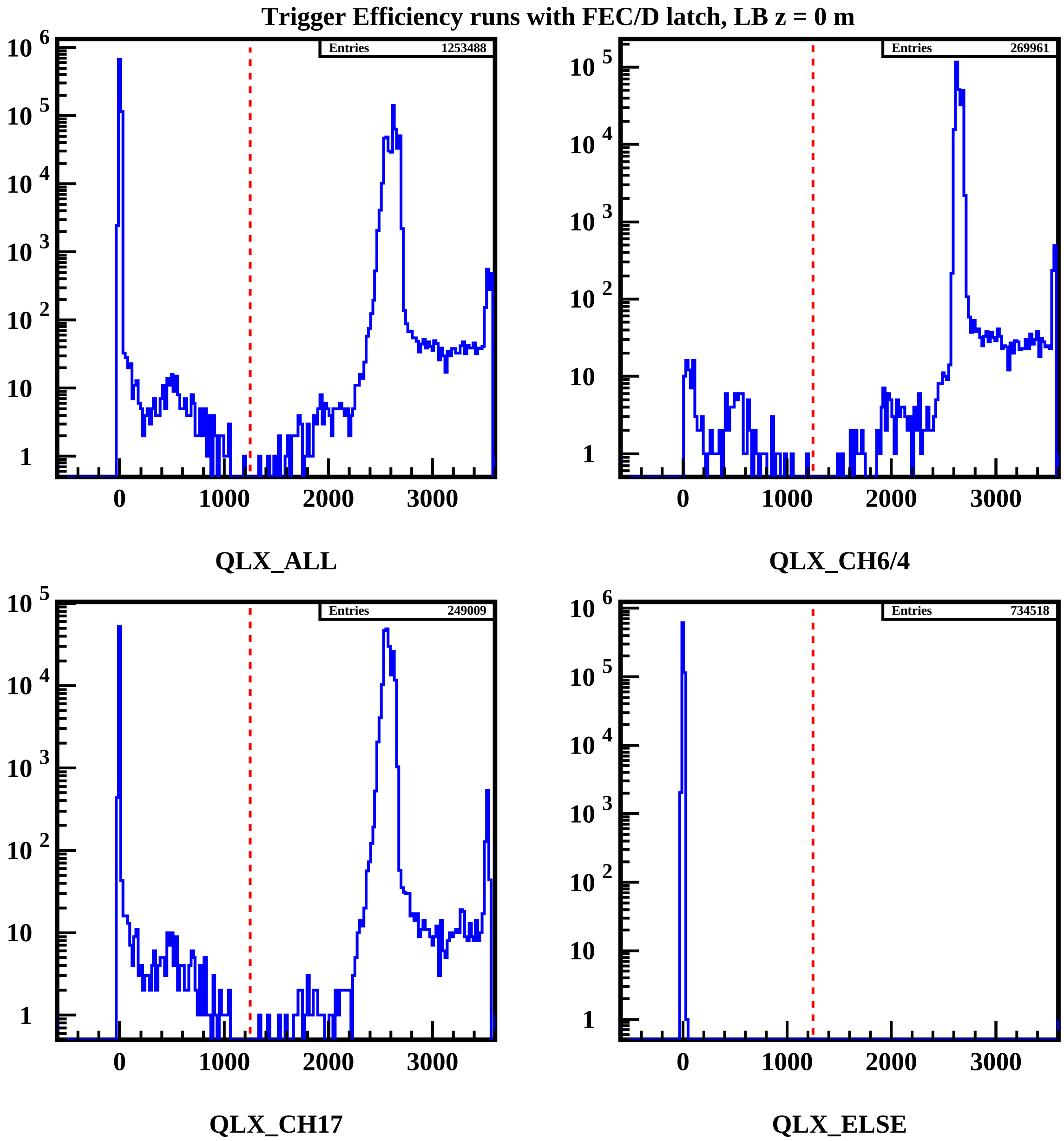

Figure 18: Pedestal subtracted QLX distributions for events in laserball trigger efficiency runs at the center of the detector. The FEC/D channels connected to raw trigger inputs (ch 4/6 and 17) are shown along with the distribution for all FEC/D channels ("ALL") and for all channels except ch 4/6 and 17 ("ELSE").

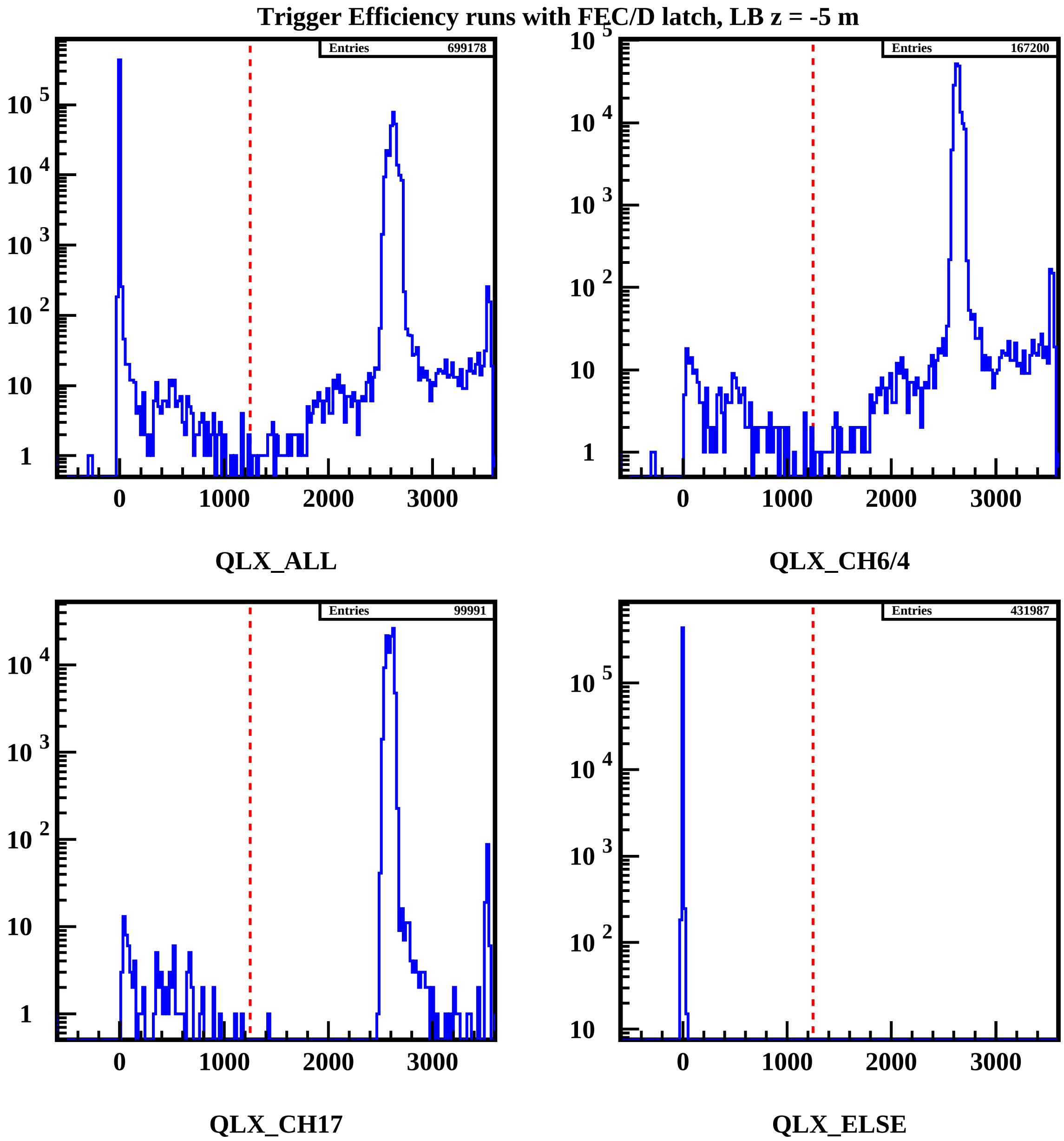

Figure 19: Pedestal subtracted QLX distributions for events in laserball trigger efficiency runs with the source at z = -5 m. The FEC/D channels connected to raw trigger inputs (ch 4/6 and 17) are shown along with the distribution for all FEC/D channels ("ALL") and for all channels except ch 4/6 and 17 ("ELSE").

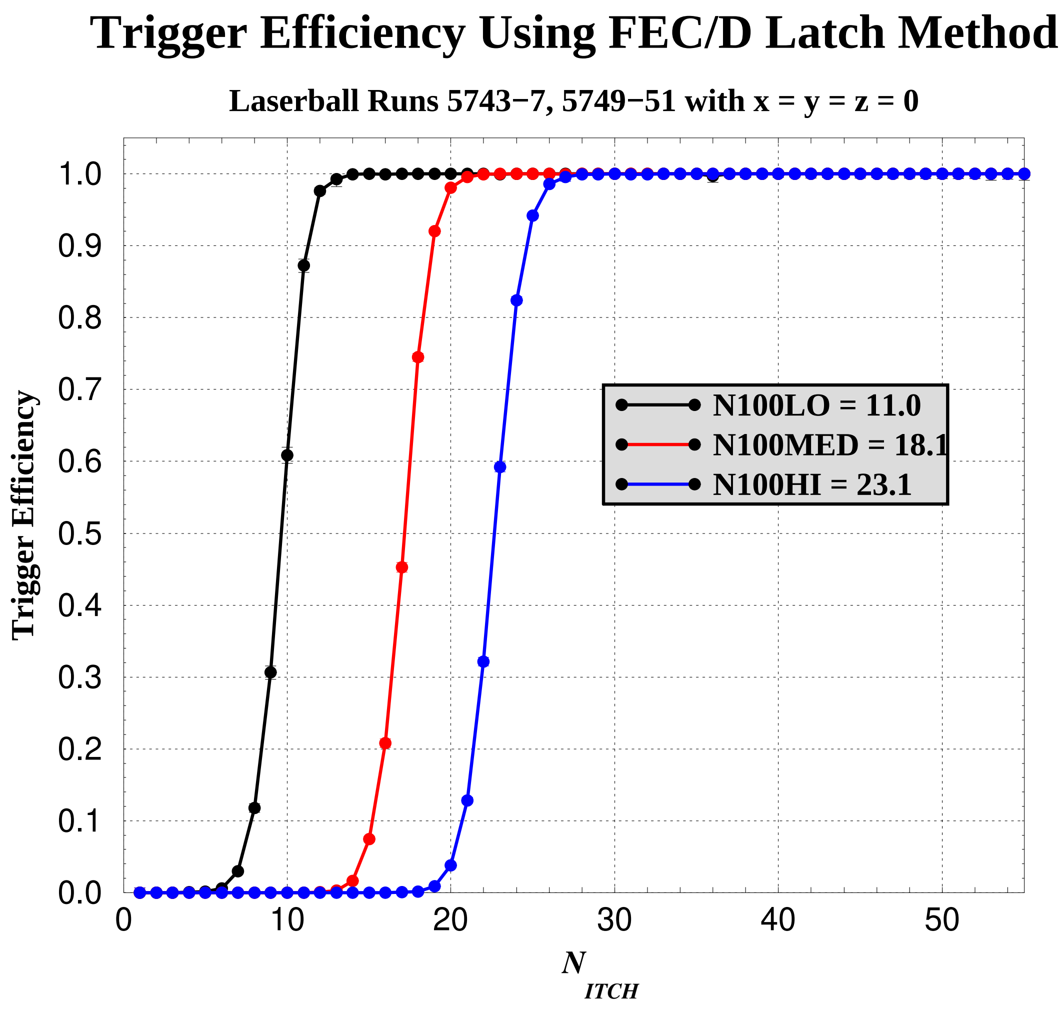

Figure 20: Measured trigger efficiency using the laserball with the FEC/D as the trigger latch. The laserball position is $x = y = z = 0$.

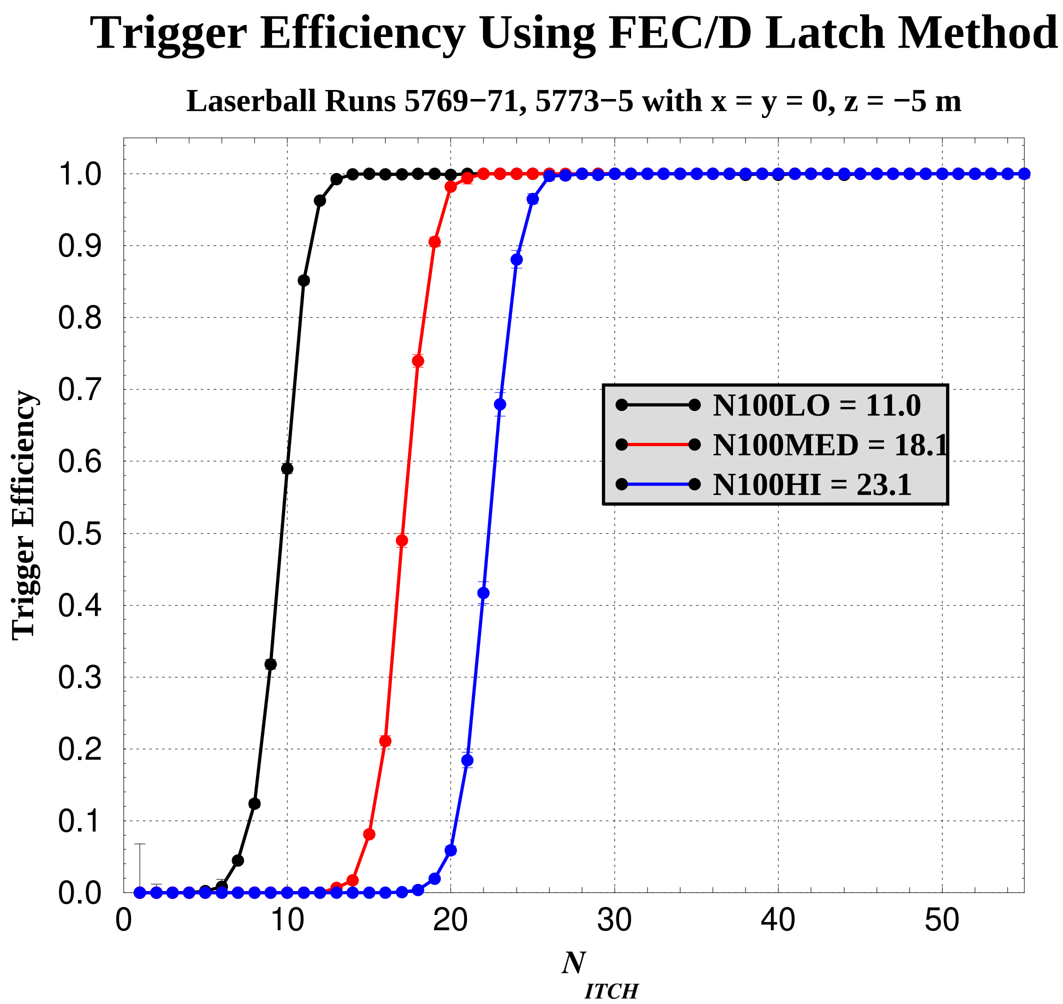

Figure 21: Measured trigger efficiency using the laserball with the FEC/D as the trigger latch. The laserball position is $x = y = 0, z = -5$ m.

-5 m, respectively. The results at the center indicate $\sim$ 3.5 NHIT turn-on for the N100L threshold and $\sim$ 3.8 NHIT turn-on for the N100MED and N100HI threshold triggers. The trigger efficiency for the laserball at z = -5 m is almost identical to the results at the center, except near threshold where the efficiency is rapidly changing and the maximum difference is between 2% and 25% for the low and high NHIT thresholds, respectively. While most prompt hits are close in-time for the laserball at the center of the detector, at z = -5 m the hits from an isotropic source are more spread out in time due to geometric effects, so this is a good test of the analog integrity of the NHIT primitives summed together trigger system. The sharper and more uniform the analog N100 primitives throughout the NHIT sum, the less position variation there will be in the NHIT trigger efficiency. Another interesting feature of the measured efficiency curves is that deviation between the NHIT hardware threshold and the 50% efficiency NHIT ($\tilde{N}$) decreases approximately linearly with $\tilde{N}$. This is most likely due in part to the changing fractional contribution of CMOS dropout to the effective threshold. Recall from the discussion of trigger inefficiencies in Section 4 that CMOS dropout leads to a *reduction* in the effective NHIT threshold which shifts the efficiency curve toward lower $\tilde{N}$ for the period of time that an offending channel is dropped out.

6.2.1 Sensitivity to In-time Channel Width

The trigger efficiency results shown in Figures 20 and 21 were generated using a sliding 93 ns time window to count the number of in-time channels in each event. The width of this window was chosen because it roughly corresponds to average length of the trigger coincidence window set by the width of the analog NHIT trigger primitives summed together in the system. Although it is natural to parameterize the trigger efficiency in this manner, one may wonder how sensitive the measured curve is to changes in the width of the in-time channel window. Figures 22 and 23 show trigger efficiency curves with the laserball source at the center and at z = -5 m, respectively, for in-time channel widths of 88, 93, and 98 ns. Note that over a 10 ns change in window width, the efficiency curves are very similar with a maximum deviation of about 10% in absolute efficiency occurring for the N100HI trigger near threshold.

The curves in Figures 22 and 23 demonstrate that we have not fine-tuned the efficiency to any particular sliding time window. However, variations in efficiency due to changes in

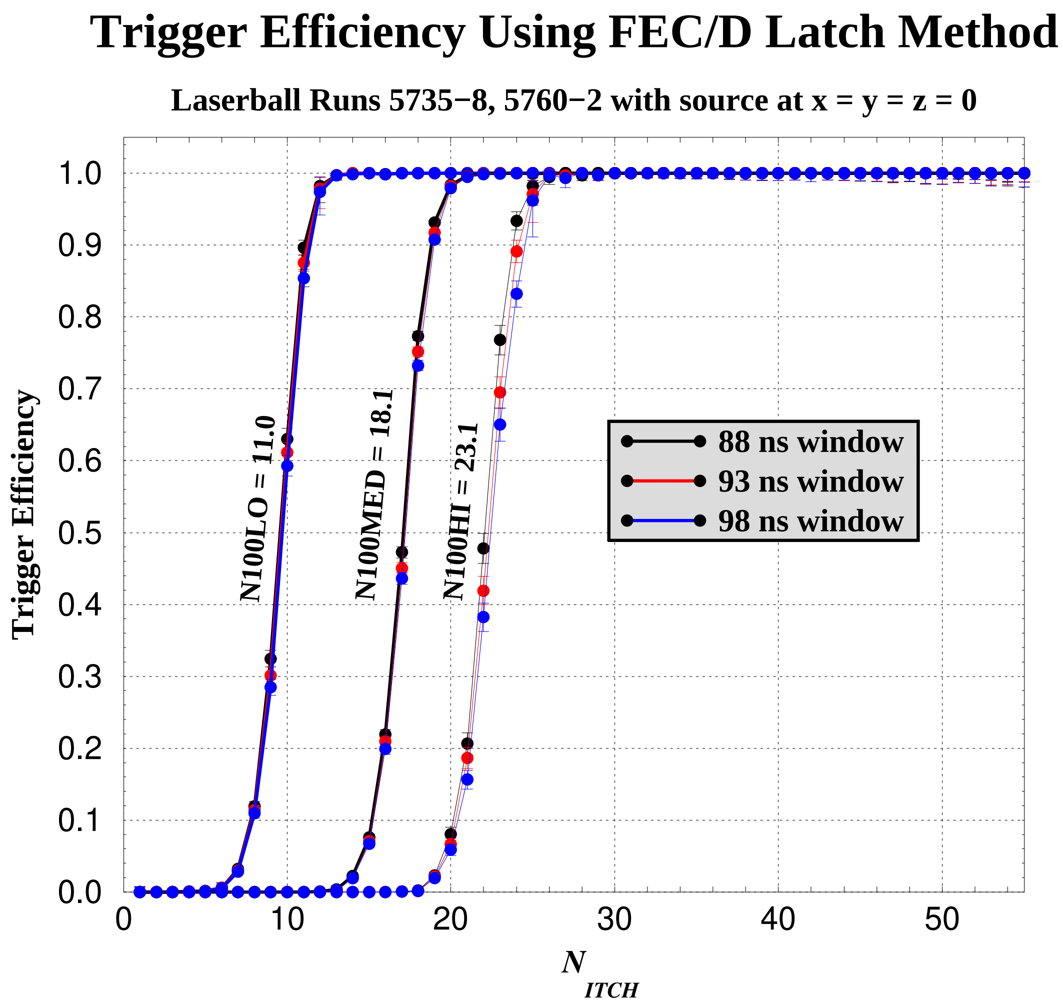

Figure 22: Effect of varying the sliding time window width used to count the number of in-time channels for the FEC/D latch method. The laserball position is $x = y = z = 0$.

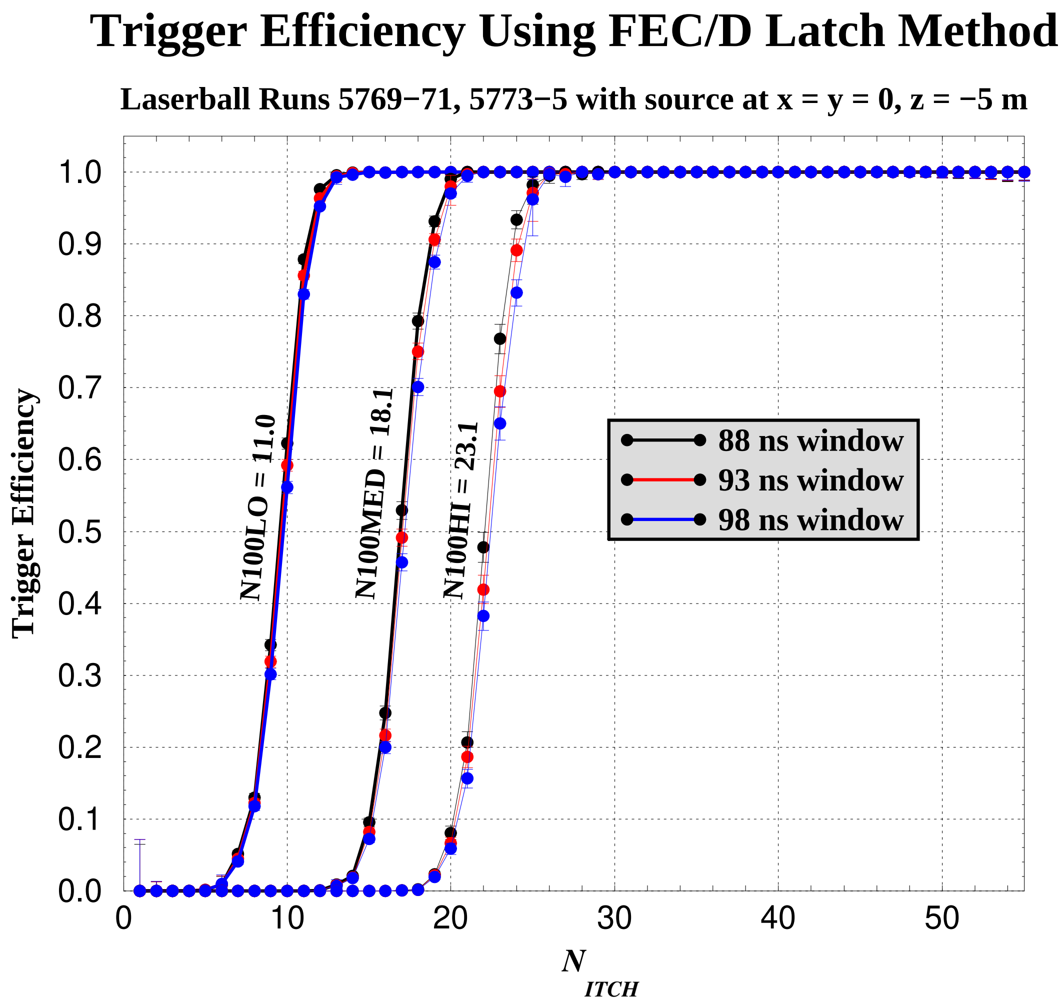

Figure 23: Effect of varying the sliding time window width used to count the number of in-time channels for the FEC/D latch method. The laserball position is $x = y = 0, z = -5$ m.

the sliding time window width should not be considered a source of systematic uncertainty in the method but rather a different way to parameterize the measured efficiency. Specifically, when the trigger efficiency curve is used to calculate the detector acceptance for a particular type of physics, one would use the *same* sliding time window to get the distribution of in-time channels. Use of the average trigger coincidence time of $\sim 93ns$ as the width of the in-time window is a convenient a way to parameterize the efficiency since channels contribute to the analog sum over this period of time and it is long enough (by design, of course) to include most hits in a normal Cerenkov event at any position in the detector.

6.2.2 Sensitivity to Timing Calibrations

Recall that full ECA/PCA timing calibrations were used in arriving at the trigger efficiency results presented in this report, and that only events with all channels passing the calibration were included in the analysis. In contrast to effects from varying the width of the in-time channel window, the accuracy of timing calibrations *does* figure into the systematic uncertainty of the trigger efficiency measurement. This is because we use calibrated channel times to count how many hits are in-time for each event, and so errors in this calibration can lead to an inaccurate determination of $\tilde{N}$, which translates into an uncertainty in the efficiency.

To investigate the sensitivity of the trigger efficiency results to timing calibrations, we compare efficiency curves with and without PCA constants applied to the data. For the range in occupancies covered by the trigger efficiency runs in this report, the PCA calibration corrects for the relative channel delays (PMT, cable, trace, etc) and discriminator walk effects. These corrections are of order $\sim$ 5 ns, so a comparison of results with and without PCA corrected channel times can be considered an estimate of the sensitivity to errors in channel timing of this order. Figures 24 and 25 show trigger efficiency curves with the laserball source at the center and at z = -5 m, respectively, for full ECA/PCA timing calibration and ECA only calibration. Note that the curves are nearly identical, with a maximum deviation of about 2% in absolute efficiency occurring for the N100HI trigger near threshold and the source at z = -5 m. The effect of the PCA calibrations on the statistics is also evident in the much smaller statistical error bars for the ECA only calibrations due to the fewer failed calibrations. The fact that the efficiency results are very similar for the

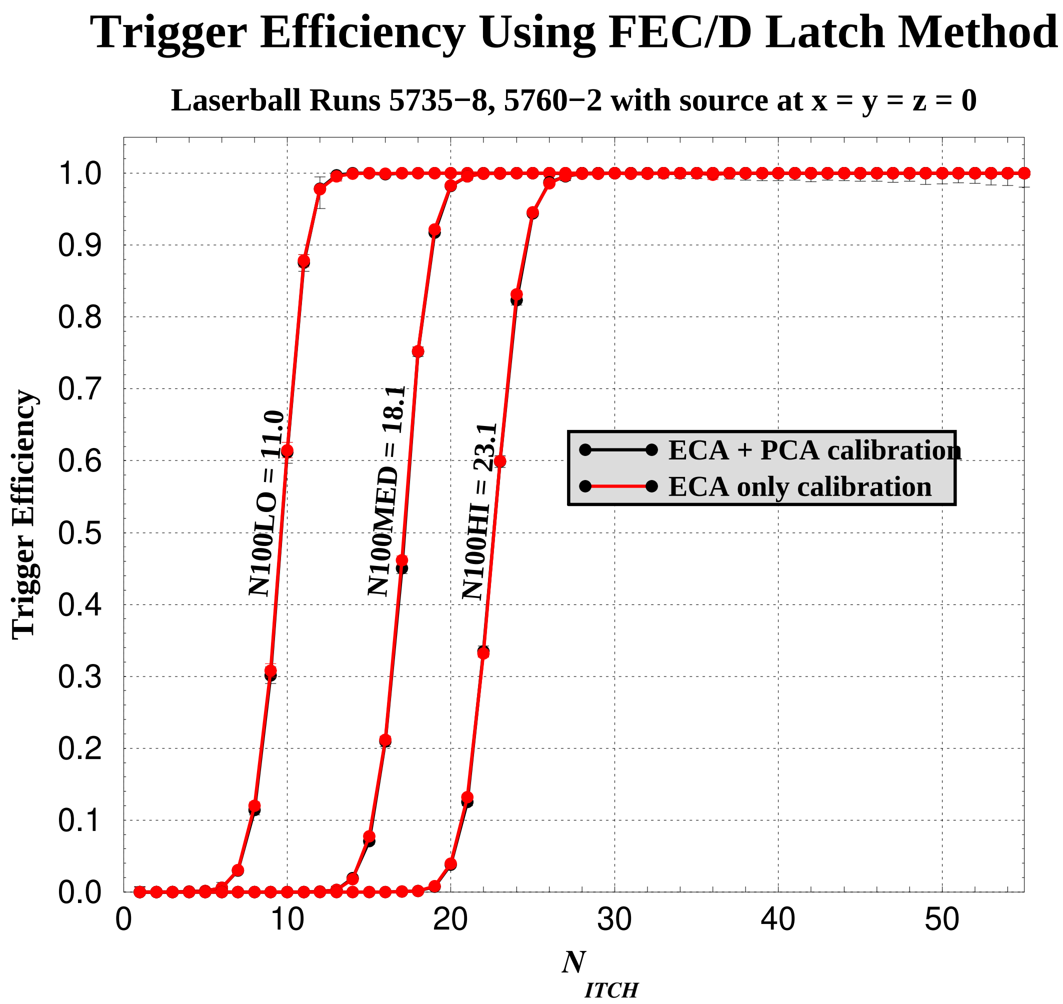

Figure 24: Effect of PCA part of the timing calibration on the trigger efficiency measured using the FEC/D latch method. The laserball position is $x = y = z = 0$.

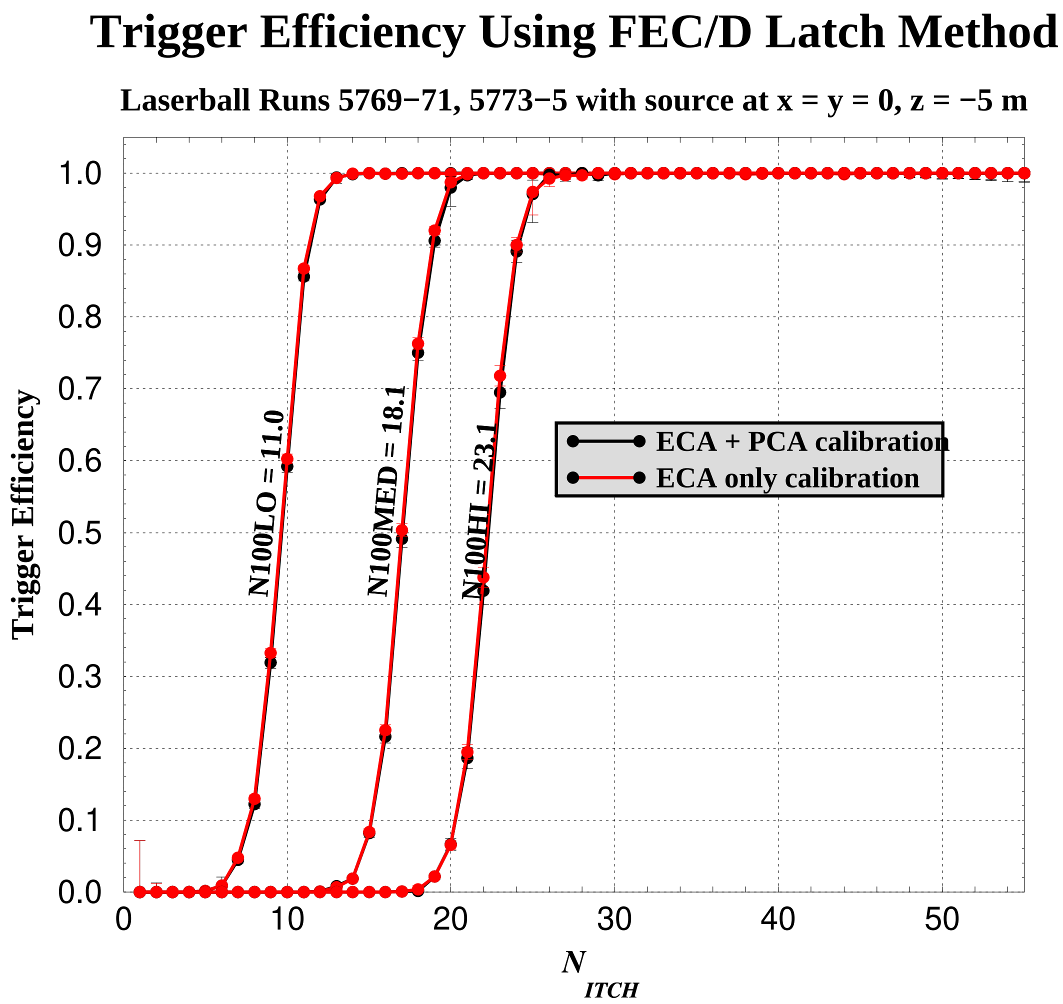

Figure 25: Effect of PCA part of the timing calibration on the trigger efficiency measured using the FEC/D latch method. The laserball position is $x = y = 0, z = -5$ m.

two types of calibrations suggests that we could revert to ECA calibrations for an event in future analyses when PCA fails on any channel without introducing much error into the measurement.

6.2.3 Sensitivity to FEC/D Charge Cut

Recall that the FEC/D trigger efficiency method uses a cut on the QLX counts above pedestal (c.a.p) of each FEC/D channel to determine which NHIT triggers fire in a given laser triggered event. The trigger efficiency at a given $\tilde{N}$ is directly related to the number of NHIT firings at that $\tilde{N}$, so the question of how sensitive the results are to changes in the charge cut position is particularly relevant to the measurement.

To see the level at which the trigger efficiency results are sensitive to the FEC/D charge cut one only needs to look at Figures 18 and 19. It can be seen that the low-gain charge integration peak is prominent on the log plots and that even a 50% change in the QLX cut value of 1250 c.a.p would result in a negligible change in the measured efficiency. For this reason, the measurement is considered robust against reasonably chosen QLX cut values, and using the FEC/D channels in this way provides a nearly unambiguous determination of the NHIT raw trigger states in each event.

To make a cleaner measurement in future FEC/D method trigger efficiency runs, one should consider a box-type cut using the high-gain charge (QHL) information as well. The problem with including QHL in analyses of FEC/D method data taken so far is that the 26 ns TTL-level raw trigger pulses tend to rail the high-gain integration and in some cases lead to a negatively railed QHL measurement. A way to avoid this in future runs is to simply attenuate the NHIT raw trigger pulses going into the FEC/D channels. This would allow confident use of both the low and high-gain charge measurements for consistency as well as reduce the cross-talk between FEC/D channels which can falsely enhance the measured efficiency.

6.2.4 Estimation of Negligible Inefficiency Points

It was previously mentioned that most early neutrino analyses in SNO will be at energies well above our hardware threshold of 18 NHIT ($\sim$ 2.3 MeV of electron energy at the center of the detector). Based on the trigger efficiency results presented in report, we might expect the

$\tilde{N}$	Laserball z (m)	Timing calibration	$\epsilon(\tilde{N})$ N100MED = 18.1	N100HI = 23.1
21	0	ECA + PCA	$0.996^{+0.003}_{-0.005}$	$0.125^{+0.005}_{-0.005}$
21	-5	ECA + PCA	$0.997^{+0.001}_{-0.006}$	$0.19^{+0.01}_{-0.01}$
21	0	ECA only	$0.9956^{+0.0007}_{-0.0007}$	$0.132^{+0.004}_{-0.004}$
21	-5	ECA only	$0.9986^{+0.0005}_{-0.003}$	$0.19^{+0.01}_{-0.01}$
22	0	ECA + PCA	$0.9992^{+0.0003}_{-0.001}$	$0.335^{+0.007}_{-0.007}$
22	-5	ECA + PCA	$1.000^{+0}_{-0.002}$	$0.42^{+0.02}_{-0.02}$
22	0	ECA only	$0.9996^{+0.0001}_{-0.0007}$	$0.332^{+0.005}_{-0.005}$
22	-5	ECA only	$1.000^{+0}_{-0.001}$	$0.44^{+0.01}_{-0.01}$
23	0	ECA + PCA	$1.000^{+0}_{-0.0004}$	$0.599^{+0.008}_{-0.008}$
23	-5	ECA + PCA	$1.000^{+0}_{-0.003}$	$0.69^{+0.02}_{-0.02}$
23	0	ECA only	$1.000^{+0}_{-0.0002}$	$0.600^{+0.006}_{-0.006}$
23	-5	ECA only	$1.000^{+0}_{-0.001}$	$0.72^{+0.01}_{-0.01}$

Table 4: Trigger efficiency results near full efficiency for the N100MED threshold using FEC/D latch method.

detector to be fully efficient at triggering on the higher energy neutrinos, but this is ultimately an acceptance question which depends only in part on the trigger efficiency. Therefore, it is important to know under what conditions the trigger system is very near 100% efficient so that contributions to the acceptance from the trigger efficiency are negligible.

Table 4 contains the numerical trigger efficiency results for the N100MED and N100HI thresholds around the number of in-time hits where the N100MED efficiency approaches unity. If we consider $\epsilon > 99.9\%$ as representing negligible inefficiency in the trigger, then it is apparent from Table 4 that the system is fully efficient (within one standard deviation) at $\tilde{N} = 22$, except possibly for ECA + PCA calibrations with the source at the center of the detector. To add a margin of safety in the results, we consider the main physics trigger for the detector - the N100MED = 18 NHIT threshold - fully efficient at $\tilde{N} = 23$ for sources within 5 m of the center.

There is an additional safety margin in the validity of the full efficiency result due to contributions from other masked in triggers. Recall from Section 2 that a global trigger is issued on the logical **OR** of all masked in trigger types, so to properly answer the relevant question - "how often does the trigger system issue a global trigger on $\tilde{N}$ channels firing in coincidence?" - one needs to consider contributions from all masked in trigger types. For example, the N100HI threshold is $\sim 60-70\%$ efficient at $\tilde{N}=23$ so we might expect that a large fraction of the medium threshold "misses" will still fire the high threshold and trigger the detector. This is a bit naive because of the strong correlation between the two thresholds - they discriminate the same analog sum so a miss of one may be correlated to a miss in the other - but the effect of the other masked in triggers can only *increase* the efficiency at a given $\tilde{N}$.

6.2.5 Effect of Missing Channels on Trigger Efficiency

In Section 4, it was pointed out that channels which acquire data but do not contribute to the trigger sum are a source of inefficiency in the trigger system. At the time the trigger efficiency data was taken, there were a number of such channels in the system which contribute to the smearing out of the efficiency curve along with the other sources of inefficiency described in Section 4. A large fraction of these channels had their triggers deliberately disabled due to excessive CMOS dropout, and some were simply dead because of some failure in the hardware. In this section, we estimate the effect of adding dead trigger channels on the full efficiency $\tilde{N}$ point reported in Section 6.2.4. This is important because the analyzer needs to know how the results presented in this report are modified by changes in the trigger hardware state corresponding to the data being analyzed.

The "dead trigger channels" relevant for studying changes in the trigger efficiency are channels which have their triggers disabled (i.e. do not contribute to the analog trigger sum) but their sequencers *enabled* which allows them to acquire data. These channels reduce the efficiency because they are included in the count of in-time channels but lower the probability for the NHIT trigger to fire since they do not contribute to the analog trigger sum. Channels which have both their triggers *and* sequencers disabled are simply "dead channels" which are sources of inefficiency to the overall acceptance much like PMTs without high voltage applied.

In the trigger efficiency runs taken on 10/25 and 10/26/99, which comprise the data for this report, there were 9719 channels enabled to acquire data (i.e. sequencers enabled) and 9307 of these channels also had their NHIT triggers enabled based on information extracted from the DQCH banks written by the DAQ. Therefore, the results in this report correspond to a 9719 channel detector with 4.2% of the triggers disabled. To estimate how much the efficiency is reduced when additional trigger channels are disabled, consider the following. There are N_{trig} total trigger channels enabled in the system when the efficiency, $\epsilon(\tilde{N})$, is measured. An *additional* fraction, f_{dead}, of these channels then have their triggers disabled and the efficiency curve changes to $\epsilon'(\tilde{N})$. An estimate of the change in efficiency at a given number of in-time channels, $\tilde{N}_o$, is given by

$$\epsilon(\tilde{N}_o) - \epsilon'(\tilde{N}_o) = f_{dead}[1 - \epsilon(\tilde{N}_o - 1)] + f_{dead}^2[1 - \epsilon(\tilde{N}_o - 2)] + \cdots$$

The i^{th} term in the sum is the probability for getting i trigger disabled hits in the event times the reduction of efficiency in having only $\tilde{N}_o - i$ in-time channels in the analog trigger sum rather than $\tilde{N}_o$. This is actually not quite right, particularly when $\tilde{N}_o$ is comparable to $f_{dead}N_{trig}$, the number of newly disabled trigger channels, which is the most likely case since this represents adiabatic changes in the detector configuration. In this case, we include the fact that a channel can not be hit twice in the same event (although a PMT can!) and a hit in a newly disabled trigger channel removes it from the population of dead trigger channels to be picked from. Therefore, we get in the limit where the fraction of good trigger channels remains the same, the following modified series

$$\epsilon(\tilde{N}_o) - \epsilon'(\tilde{N}_o) = f_{dead}[1 - \epsilon(\tilde{N}_o - 1)] + f_{dead}(f_{dead} - \tfrac{1}{N_{trig}})[1 - \epsilon(\tilde{N}_o - 2)] + \cdots,$$

which can be written in a more compact form as

$$\epsilon(\tilde{N}_o) - \epsilon'(\tilde{N}_o) = \sum_{i=1}^{min(\tilde{N}_o, f_{dead}N_{trig})} \{\prod_{j=1}^{i} (f_{dead} - \tfrac{j-1}{N_{trig}})[1 - \epsilon(\tilde{N}_o - i)]\}$$

The $min(\tilde{N}_o, f_{dead}N_{trig})$ upper limit is included to terminate the sum when contributions from all the dead trigger channels have been included.

The results of calculating the previous sum with $N_{trig} = 9307$ are shown in Figure 26 for $\tilde{N}_o = 18$ and $\tilde{N}_o = 23$. Note that while the reduction in efficiency is substantial at $\tilde{N}_o = 18$ where the efficiency changes rapidly, the full efficiency is nearly unaffected even with relatively large fractions of the triggers disabled. This is because at $\tilde{N}_o = 23$ it takes several random chance hits of the dead trigger channels to make a substantial change in the

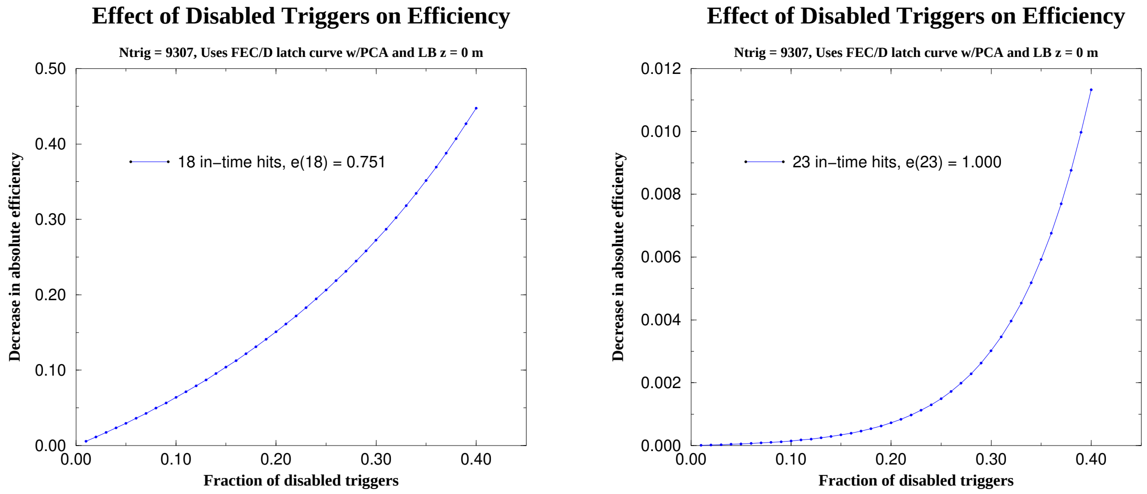

Figure 26: Reduction in efficiency versus the fraction of newly disabled trigger channels for $\tilde{N}_o = 18$ (left) and $\tilde{N}_o = 23$ (right).

efficiency (recall Figure 20) which is unlikely when only a small fraction of the good trigger channels are disabled.

It should be noted that this approximation assumes that channels are hit at random. This would be a good approximation for isotropic light at the center of the detector and the dead trigger channels were distributed uniformly over the PSUP. However, in reality, dead trigger channels are strongly correlated to certain channels that are prone to excessive CMOS dropout and hence the PMTs connected to them have a non-uniform distribution on the PSUP which complicates the estimate. Still, the equation presented in this section should give a rough estimate of the effect of disabling trigger channels on the trigger efficiency.

6.3 Comparison with Pulsed Global Trigger Inferred Rates

As mentioned in Section 2, we trigger the detector at a constant 5 Hz rate to collect information about the status of the detector at regular intervals. The resulting PULSE_GT events are useful because they provide regular "snapshots" of the system, independent of any light in the detector. The PULSE_GT data is particularly useful for trigger efficiency because it provides a way of getting an *unbiased estimate of the rate of in-time channels*

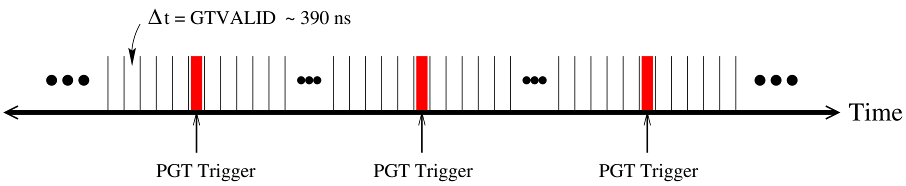

Figure 27: Diagram showing how time can be thought of as being divided into GTVALID width bins that PULSE_GT triggers periodically sample to count the average number of hits in each bin.

occurring in the system. This rate function, when convolved with a trigger efficiency curve for a given trigger threshold, leads to a prediction about the rate at which the system will trigger on that threshold. This rate can be compared to actual trigger rate observed when the particular trigger type is masked in to generate global triggers.

In this section, we estimate the rate of in-time channels, $R(\tilde{N})$, from the PULSE_GT data and convolve this with the trigger efficiency curve measurement, $\epsilon(\tilde{N})$, presented in Section 6.2 for the N100MED = 18.1 threshold to arrive at an estimate of the expected trigger rate, R^{100M}_{exp}. We then look at the consistency between this PULSE_GT inferred rate and the N100MED trigger rate, R^{100M}_{obs}, observed in the production neutrino data over the same period of time.

During a PULSE_GT event, or any other global trigger for that matter, all channels which fired less than GTVALID $\sim$ 390 ns before the arrival of the global trigger signal at the front-end are collected into the event[7]. Therefore, each PULSE_GT trigger can be thought of as opening a time window of GTVALID width and counting the number of hit channels in that window. In fact, to understand how $R(\tilde{N})$ is determined from the PULSE_GT data, its best to think of all time divided up into GTVALID width bins that the PULSE_GT trigger samples at a regular rate (see Figure 27). If we then slide a 93 ns window around the PMT times of each PULSE_GT event to get $N(\tilde{N})$, the number of events having $\tilde{N}$ in-time channels (determined by the maximum number in any window), then the rate of $\tilde{N}$ is given

[7]The alert reader may have flipped back to Figure 15 at this point and noticed that the PMT times only span (3600 - 400 counts) / 8.6 $\sim$ 370 ns. This is because the of the “TAC curl” which maps the last $\sim$ 20 ns of the TAC ramp (i.e. early hits) back to 3600 ADC counts and below.

by

$$R(\tilde{N}) = \frac{N(\tilde{N})}{(N_{PGT})(GTVALID)},$$

where N_{PGT} is the total number of PULSE_GT triggers considered. The expected N100M trigger rate is then estimated by convolving $R(\tilde{N})$ with the measured efficiency, $\epsilon(\tilde{N})$, to give

$$R_{exp}^{100M} = \sum_{\tilde{N}=0}^{\infty} \epsilon(\tilde{N})R(\tilde{N})$$

Substituting for $R(\tilde{N})$, the rate of in-time channels from the PULSE_GT data, in the previous relation gives

$$R_{exp}^{100M} = \frac{1}{(N_{PGT})(GTVALID)} \sum_{\tilde{N}=0}^{\infty} \epsilon(\tilde{N})N(\tilde{N})$$

for the expected N100M trigger rate based on the PULSE_GT data and the measured trigger efficiency for this threshold.

The PULSE_GT data used in the analysis of this section was extracted from production neutrino runs 10000 - 10237. Events having the PULSE_GT bit set in the trigger word were selected but not if the PED bit was also set to avoid catching events from the NHIT monitoring DAQ task. In addition, only events with $NHIT \geq 10$ were included to avoid windowing around the PMT time spectrum of a large number of events that contribute a negligible amount to the N100M trigger rate, since the measured efficiency is zero for all practical purposes below an $\tilde{N}$ of 10 channels[8]. The resulting NHIT spectrum of selected PULSE_GT events is shown in Figure 28 along with the distribution of in-time channels after the 93 ns sliding window is applied to the PMT time spectrum of events. As shown in the figure, 5576 events survived the NHIT cut out of 8819747 total PULSE_GT events (after events with the PED bit set in the trigger word were removed). Note that the blue curve in Figure 28 is $N(\tilde{N})$, so we are ready to convolve this distribution with the N100M = 18 trigger efficiency measured using the laserball with FEC/D latch method and shown in Figure 20[9]. Table 5 shows the individual terms that are summed together to get 18.96 for the mean number of N100M triggers we expect from the distribution of in-time channels in

[8] and NHIT is guaranteed to be larger than $\tilde{N}$.

[9] We use the laserball run at the center of the detector for simplicity.

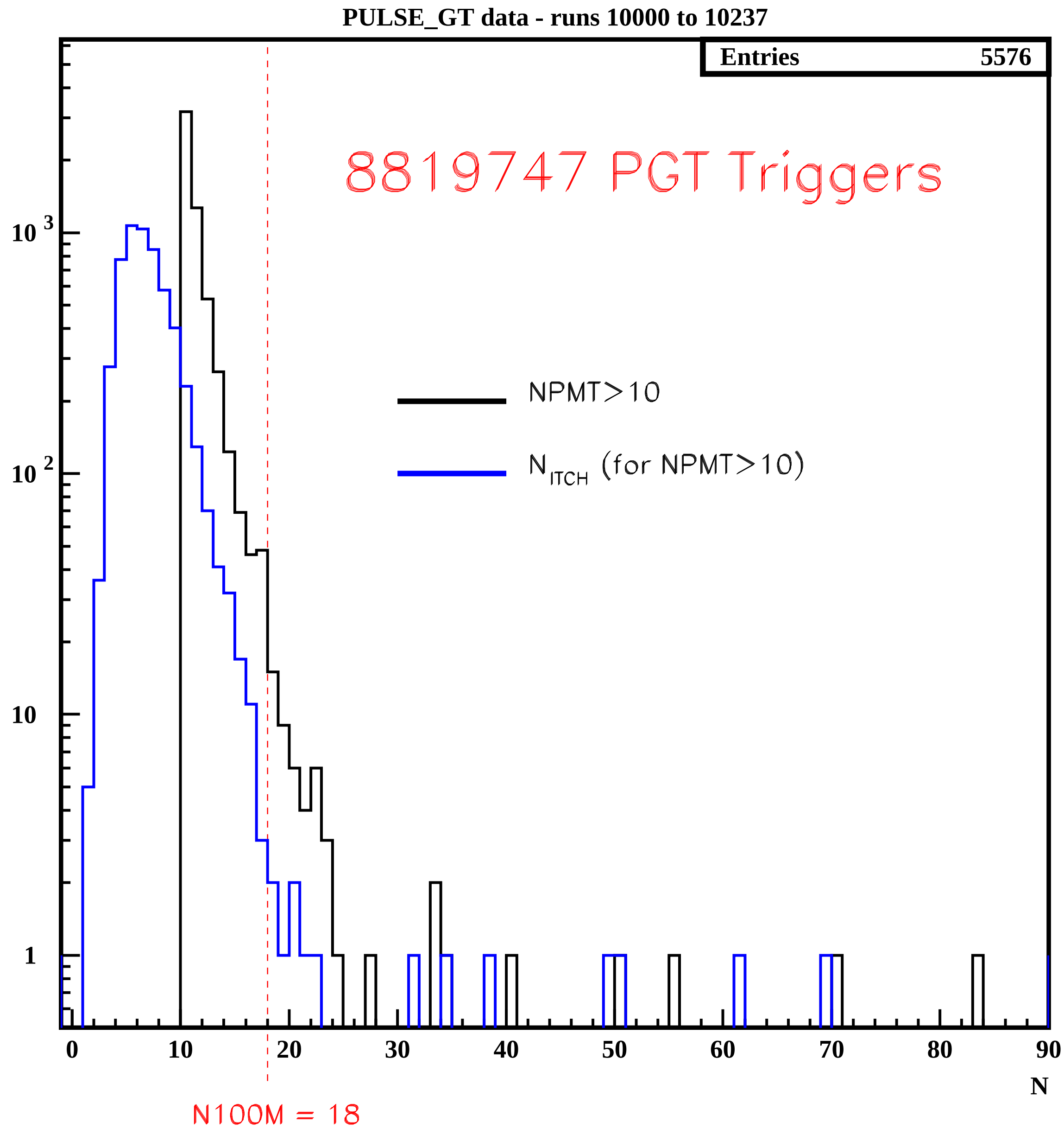

Figure 28: NHIT distribution of PULSE_GT events cut from runs 10000 to 10237 with $NHIT > 10$. Also shown is the distribution of the maximum number of hits in any 93 ns sliding window applied to PMT time distribution of each PULSE_GT event.

$\tilde{N}$	$\epsilon(\tilde{N})$	$N(\tilde{N})$	$\epsilon(\tilde{N})N(\tilde{N})$
< 12	0	–	0
12	0.00044	70	0.03
13	0.0026	41	0.11
14	0.012	32	0.59
15	0.074	17	1.26
16	0.21	11	2.31
17	0.45	3	1.35
18	0.74	2	1.48
19	0.92	1	0.92
20	0.98	2	1.96
> 20	1.00	9	9
	$\sum_{\tilde{N}=0}^{\infty} \epsilon(\tilde{N})N(\tilde{N}) =$		18.96

Table 5: Table showing the convolution of the measured trigger efficiency curve for N100MED = 18 and the rate of in-time channels estimated from PULSE_GT.

the PULSE_GT data set and the measured trigger efficiency. Substituting this value as well as $N_{PGT} = 8819747$ and $GTVALID = 390$ ns with approximate errors into the relation for the expected N100M trigger rate, we get

$$R^{100M}_{exp} = \frac{18.96 \pm \sqrt{18.96}}{(8819747)(390 \pm 30 \times 10^{-9})} \text{ Hz} = 5.5 \pm 1.6 \text{ Hz}$$

In order to compare the expected result to the actual N100M trigger rate, the rate of events from runs 10000 - 10237 having the N100M bit set in the trigger word was recorded in 10 minute intervals. The results are shown in Figure 30, where it can be seen that the rate was fairly erratic over the 500 hour period. The average N100M trigger rate over this period is

$$R^{100M}_{obs} = 6.9 \pm 3 \text{ Hz}$$

which is consistent with the rate obtained from PULSE_GT data and the measured trigger efficiency.

It should be noted that there are corrections to the expected NHIT trigger rate using PULSE_GT data due to coincidences with other masked in triggers. The problem is that

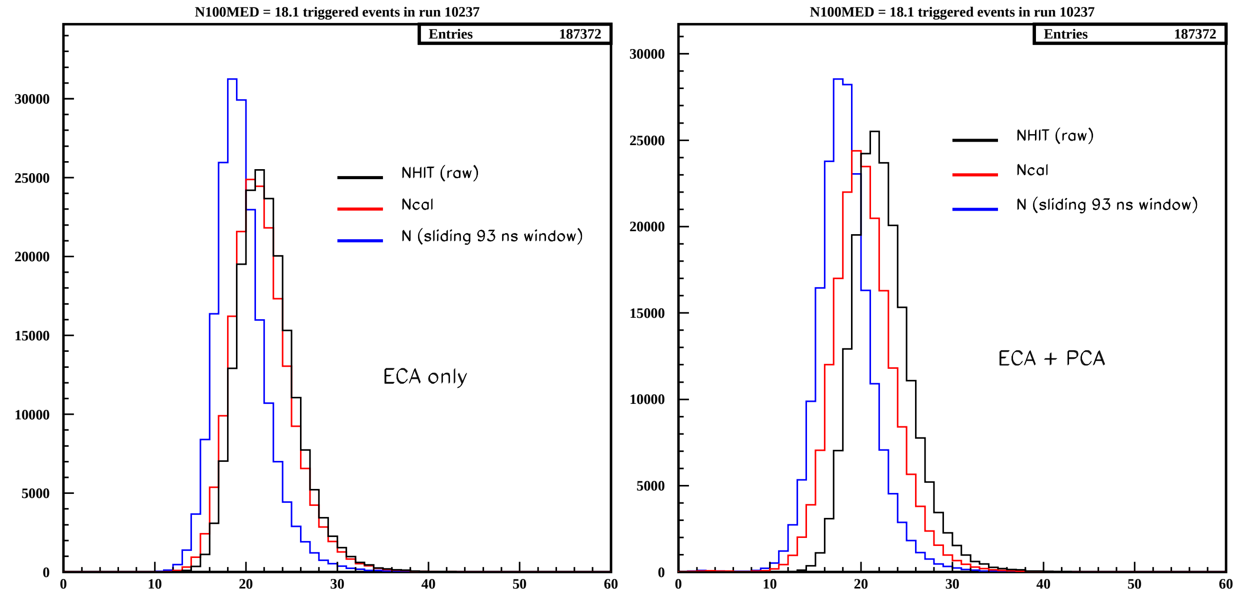

Figure 29: NHIT distribution of all events (black) and events having all hits passing the timing calibration (red) for N100MED triggered events in run 10237. Also shown (blue) is the distribution of $\tilde{N}$, the maximum number of hits in a sliding 93 ns time window.

other masked in triggers which arrive at the global trigger generation logic just *before* the pulser generated raw trigger signal will generate a global trigger and lockout the PULSE_GT trigger.[10] This effect would be a benign loss of data if it was not for the fact that these other masked in trigger types have non-uniform NHIT distributions and hence the probability for another trigger to "steal" a PULSE_GT trigger is correlated to the NHIT of the event. This results in a distortion of the spectrum shown in Figure 28 and leads to corrections in the estimate of the rate of in-time channels occurring in the detector based on PULSE_GT data. The most significant contributer to this distortion would be from the N100MED trigger, which as we mentioned has an average rate close to the PULSE_GT rate and an NHIT spectrum shown in Figure 29. While one can calculate the distortion from the coincidence probability based on the PULSE_GT and N100MED rate, its a bit undesirable to use the measured N1000MED rate in a correction to the calculation of the expected N100MED

[10]Recall from Section 2 that there is LOCKOUT period of $\sim$ 440 ns after a global trigger is issued until another global trigger can be generated.

rate. Instead, one should consider looking for the absence of PULSE_GT triggers at integer multiples of pulser period (200 ms) and determining what masked in trigger type caused the miss as well as the $\tilde{N}$ of the event to correct for the rate of in-time channels estimation. Future analyses comparing the PULSE_GT expected trigger rate to observed rates should include such corrections to more precisely constrain the trigger efficiency.

The type of comparison presented in this section is quite useful for an independent check on the gross features of the measured trigger efficiency. For a more precise comparison between the two rates, a much larger PULSE_GT data set would be needed and a smaller spread in the NHIT trigger rate in addition to the corrections already mentioned. This could be obtained using data from a high rate PULSE_GT run (e.g. the system can handle a few hundred Hz of PULSE_GT since it is low occupancy) with the desired NHIT trigger masked in as well. This would allow a simultaneous determination of the rate of in-time channels (from PULSE_GT) and the NHIT trigger rate over a time scale much less than 500 hours which should yield a smaller variance in the NHIT rate.

7 Conclusions and Recommendations

The efficiency of the 100 ns NHIT trigger was measured using the laserball as a source of in-time hits and FEC/D calibration channels to determine how often the trigger fires in response to these hits. Measurements were performed on the three different thresholds used in production neutrino data taking with 9307 trigger channels enabled in the system. It was found that the efficiency curves have a turn-on (10% to 90%) of between 3.5 and 3.8 NHIT and the *shapes* of the curves for each threshold are very similar. The dependence of the efficiency on source position is largest near threshold where the efficiency is rapidly changing and the maximum difference is found to vary between 2% and 25% for the low and high NHIT thresholds, respectively, as the source is moved from the center of the detector to z = -5 m. The medium NHIT threshold (N100MED = 18.1), which is the main physics trigger for the detector, is found to be > 99.9% efficient when there are 23 or more hits within 93 ns coincidence (i.e. $\tilde{N} \geq 23$ NHIT). This corresponds to $\sim$ 2.9 MeV of electron energy at the center of the detector using a very rough energy calibration of 8 hits/MeV. This result is unchanged when the laserball source position is moved from the center of the

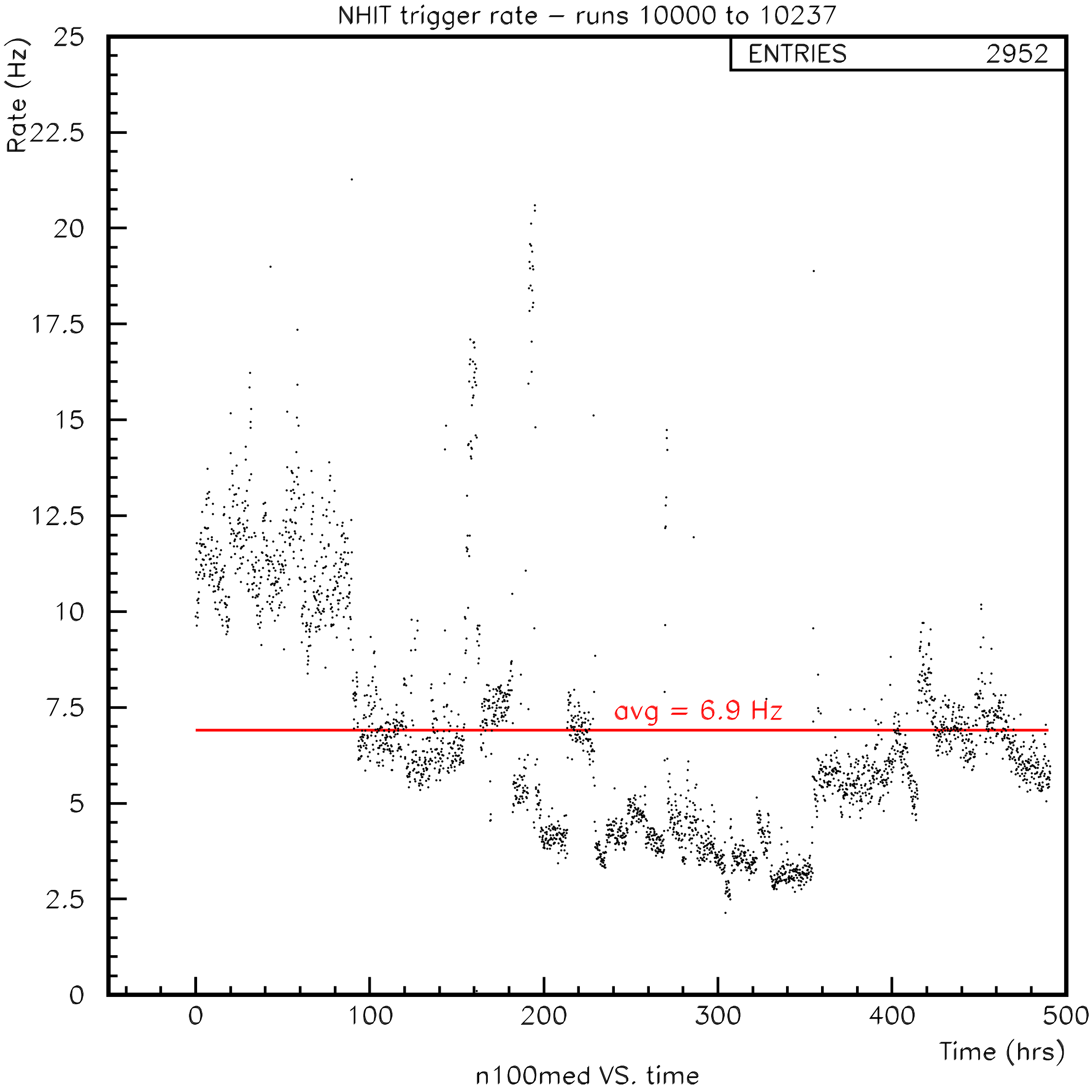

Figure 30: The N100MED trigger rate in 10 minute intervals over runs 10000 - 10237. The average rate over this period was 6.9 ± 3 Hz.

detector to z = -5 m and is found to be robust against modest changes in the number of enabled trigger channels. In particular, it was estimated that the system would remain fully efficient for $\tilde{N} \geq 23$ NHIT even if an additional 20% of the trigger channels - on top of the already disabled 4.2% of the total - were disabled. This statement is not meant to encourage frivolous disabling of trigger channels since this can lead to other problems (e.g. create dead areas which ultimately complicates estimates of acceptance), but rather to demonstrate that the full efficiency region is robust against small changes in the trigger configuration of the detector.

Several systematic checks of the trigger efficiency results were performed. The sensitivity of the results to the width of the sliding time window used to count the number of in-time channels was investigated and it was found that the maximum absolute change in efficiency is $\sim$ 10% when the width is changed by roughly 10% around the 93 ns nominal value, however the majority of changes are much smaller. It was pointed out that changing the width of the in-time channel window really represents a different way to parameterize the efficiency rather than a systematic error, however, it is important to check that the results are not finely-tuned to a particular choice of window width. The sensitivity of the results to changes in timing calibrations and position of the FEC/D charge cut was also considered and found to have very little effect on the efficiency curve. In particular, the maximum change in efficiency when the PCA timing calibration is applied (which corrects for transit time differences on order of 5 ns) is found to be $\sim$ 2% in absolute efficiency. In addition, an inspection of the QLX distributions for FEC/D channels connected to the NHIT raw trigger outputs suggests that the results are robust against large (50% or so) changes in the position of the QLX charge cut. The trigger efficiency results were also found to be roughly consistent with the approximate MTC/D latch methods using both laserball calibration data and normal NHIT triggered data collected over a period of production neutrino data taking. Finally, the expected NHIT trigger rate inferred from pulsed global trigger data *and* the measured trigger efficiency was found to be consistent with the observed NHIT trigger rate measured over the same period of time.

There are several recommendations which follow from the results of this report. There should be more data taken using the FEC/D latch method to check the main results of this report and to track changes in the efficiency over time. This body of new data should include laserball source runs outside 5 m and as close to the PSUP as possible to fully test the position dependence. We also recommend several changes in the FEC/D latch method for future data taking. First of all, one should use all existing hardware to measure four triggers at once (e.g. three NHIT100 thresholds and one NHIT20) which will help make the data acquisition and analysis more efficient. Also, the TTL-level raw trigger pulses should be attenuated before going into the FEC/D to reduce pickup and crosstalk between channels and to allow high-gain charge information to be confidently used as a cross-check of the low-gain charge measurement.

More work should be done in using NHIT triggered data to accurately determine the trigger efficiency. An extension of the NHIT triggered MTC/D latch method described in this report would be valuable for tracking changes in the trigger efficiency using the production neutrino data stream. This method is potentially very useful since it does not require any disruption in normal taking and allows continuous monitoring of the efficiency over time. In addition, some thought should be given to the using the FEC/D channels in measuring the trigger efficiency during NHIT triggered data taking. One could trigger on the medium NHIT100 threshold and plug one or more of the other thresholds into FEC/D channels for measurement. This would allow a more robust determination of how often the NHIT triggers fire in response to in-time hits without the use of the laserball, however one would need to investigate the FEC/D channel timing since we do not have control of the trigger delay like in the laserball method (unless cable delay was added to the N100MED raw trigger).

Once the trigger efficiency results are blessed (whether they are curves shown in this report or results based on future measurements), they should get incorporated into the Monte Carlo trigger simulation for general use. Once these curves characterizing the trigger hardware response are in SNOMAN and the MC has been calibrated (e.g. optical calibration input gives energy response matching calibrations), one can begin studying acceptance, although as previously mentioned, most early SNO analyses will be in a regime where contributions from the trigger efficiency are trivial. In addition, work is underway to include a processor (TRF) in SNOMAN which will allow "automatic" generation of trigger efficiency tables in the form of titles banks when new trigger efficiency data is collected.

A Error Determination

The trigger efficiency measurement is inherently a binomial measurement - in each of N trials, the trigger either fires or it does not. For a binomial distribution with known success probability p, the spread (variance) in the number of observed successes, r, after N independent measurements, is given by

$$\sigma_r^2 = Np(1-p)$$

This formula could be used to calculate the trigger efficiency errors except for the small problem that if p was known, there would be no need for this report, since p *is* the trigger efficiency. However, we can use the measured trigger efficiency, $\hat{\epsilon} = \frac{r}{N}$, to estimate the true trigger efficiency ϵ (or success probability, p) and plug this into the equation for the binomial variance so that

$$\hat{\sigma}_r^2 = N\hat{\epsilon}(1-\hat{\epsilon})$$

Constructing an estimator for the variance in this way seems reasonable, however there is no guarantee that this estimator will be free of bias (i.e. $E(\hat{\sigma}_r^2) = \sigma_r^2$). An unbiased estimator of the variance for a binomial distribution is given by [2],

$$\hat{\sigma}_r^2 = \frac{N}{N-1}N\hat{\epsilon}(1-\hat{\epsilon})$$

Note that the difference between the two estimators is small for large N. This represents the spread in the observed number of successes, so we use as an estimate for the 1σ error on the trigger efficiency

$$\hat{\sigma}_\epsilon = \frac{\hat{\sigma}_r}{N},$$

where

$$\hat{\sigma}_r = \sqrt{\frac{N}{N-1}N\hat{\epsilon}(1-\hat{\epsilon})} \text{ and } \hat{\epsilon} = \frac{r}{N}$$

A problem arises in using the above form for the trigger efficiency error when we are the at or near the physical bounds of the curve (i.e. when $\hat{\epsilon} = 0$ or $\hat{\epsilon} = 1$). In both these cases, we would calculate $\hat{\sigma}_\epsilon = 0$ from our previous error relation, independent of the number of observations. This is simply because if the binomial probability actually *is* 0 or 1, then the spread in observed successes is zero. Of course, there *is* some degree of statistical uncertainty in our measurement near these bounds, particularly when N is small, so we need a way to include this into our error estimate. In fact, when $\hat{\epsilon} = 1$ ($\hat{\epsilon} = 0$) we can only place a limit on the trigger efficiency such that at a particular confidence level, the efficiency is larger (smaller) than some value. A method of constructing confidence intervals with proper coverage for Poisson processes near a physical boundary is presented in the famous paper by Cousins and Feldman [3], and the tabulated confidence intervals in Table 6 are used in calculating the trigger efficiency limits near $\hat{\epsilon} = 0$ and $\hat{\epsilon} = 1$.

B Results on the 20 ns Trigger Efficiency

Although not central to this report, the 20 ns trigger efficiency was investigated in the process of measuring the 100 ns efficiency. Recall from the runs listed in Table 3 that the N20 threshold was measured using the laserball with FEC/D latch method of Section 5.2. The analysis methods used in determining the NHIT20 trigger efficiency were identical to the FEC/D method for the 100 ns trigger except for two rather obvious differences:

- A sliding 20 ns time window was used to determine $\tilde{N}$ rather than 93 ns.
- FEC/D channel 17 connected to the N20 raw trigger output for the N20/100L runs indicated in Table 3 was used to determine in the N20 trigger fired in a given event (with the same QLX cut).

The NHIT20 trigger efficiency results for laser source position at the center of the detector and at z = -5 m are shown in Figure 31. The efficiency curve for the source at the center has an NHIT turn-on of $\sim$ 4 NHIT and we are $>$ 99.9% efficient for this threshold at $\tilde{N} = 20$ NHIT. Aside from a broader turn-on of the curve, an important qualitative difference between Figure 31 and the 100 ns trigger efficiency results shown in Figure 20 is that the N20 hardware threshold (17 NHIT) appears to be further from 50% efficiency (toward larger efficiency) than the equivalent N100 threshold. Recall from the results of Section 6.2 that the deviation between the NHIT hardware threshold and the 50% efficiency NHIT ($\tilde{N}$) decreased approximately linearly with $\tilde{N}$, which was attributed to the fractional contribution of CMOS dropout to the effective threshold (and hence efficiency). A rough interpolation of the N100

$n_0\backslash b$	0.0	0.5	1.0	1.5	2.0
0	0.00, 1.29	0.00, 0.80	0.00, 0.54	0.00, 0.41	0.00, 0.41
1	0.37, 2.75	0.00, 2.25	0.00, 1.75	0.00, 1.32	0.00, 0.97
2	0.74, 4.25	0.44, 3.75	0.14, 3.25	0.00, 2.75	0.00, 2.25
3	1.10, 5.30	0.80, 4.80	0.54, 4.30	0.32, 3.80	0.00, 3.30
4	2.34, 6.78	1.84, 6.28	1.34, 5.78	0.91, 5.28	0.44, 4.78
5	2.75, 7.81	2.25, 7.31	1.75, 6.81	1.32, 6.31	0.97, 5.81
6	3.82, 9.28	3.32, 8.78	2.82, 8.28	2.32, 7.78	1.82, 7.28
7	4.25,10.30	3.75, 9.80	3.25, 9.30	2.75, 8.80	2.25, 8.30
8	5.30,11.32	4.80,10.82	4.30,10.32	3.80, 9.82	3.30, 9.32
9	6.33,12.79	5.83,12.29	5.33,11.79	4.83,11.29	4.33,10.79
10	6.78,13.81	6.28,13.31	5.78,12.81	5.28,12.31	4.78,11.81
11	7.81,14.82	7.31,14.32	6.81,13.82	6.31,13.32	5.81,12.82
12	8.83,16.29	8.33,15.79	7.83,15.29	7.33,14.79	6.83,14.29
13	9.28,17.30	8.78,16.80	8.28,16.30	7.78,15.80	7.28,15.30
14	10.30,18.32	9.80,17.82	9.30,17.32	8.80,16.82	8.30,16.32
15	11.32,19.32	10.82,18.82	10.32,18.32	9.82,17.82	9.32,17.32
16	12.33,20.80	11.83,20.30	11.33,19.80	10.83,19.30	10.33,18.80
17	12.79,21.81	12.29,21.31	11.79,20.81	11.29,20.31	10.79,19.81
18	13.81,22.82	13.31,22.32	12.81,21.82	12.31,21.32	11.81,20.82
19	14.82,23.82	14.32,23.32	13.82,22.82	13.32,22.32	12.82,21.82
20	15.83,25.30	15.33,24.80	14.83,24.30	14.33,23.80	13.83,23.30

Table 6: 68.27% C.L. intervals for the Poisson signal mean μ, for total events observed n_0, for known mean background b ranging from 0 to 2,taken from the paper by Cousins and Feldman. The zero background (left-most) column is used in the calculation of trigger efficiency limits near the physical boundaries.

curves in Figure 20 suggests $\sim$ 75% for the expected N20 = 17.0 threshold efficiency at $\tilde{N} = 17$ compared to the measured value of 95%. This is most likely due to the dropout-induced baseline shift being a bit worse for the 20 ns trigger sum. This is consistent with recollections about the degree of CMOS dropout in comparison of the 20 ns and 100 ns trigger sums on the scope as well as how more attention was paid to disabling 100 ns triggers on channels having particularly bad CMOS dropout.

It is also evident from Figure 31 that the position dependence is a bit stronger for the 20 ns trigger than the 100 ns trigger. Recall that moving the laserball source away from the center of the detector spreads out the timing of the prompt PMT hits and provides a more stringent test of the NHIT trigger sum analog characteristics. The 20 ns NHIT pulse shape is a bit worse than the 100 ns trigger in terms of rise/fall time of the analog primitives which is a probable source of the degraded turn-on and position dependence relative to the N100 triggers.

References

[1] J. Klein, M. Neubauer, R. van Berg, and F. M. Newcomer, SNO technical report SNO-STR-97-036, University of Pennsylvania (unpublished).

[2] W. Eadie, *Statistical Methods in Experimental Physics* (North Holland, Amsterdam, 1971).

[3] G. Feldman and R. Cousins, Physical Review **D57**, 3873 (1998).

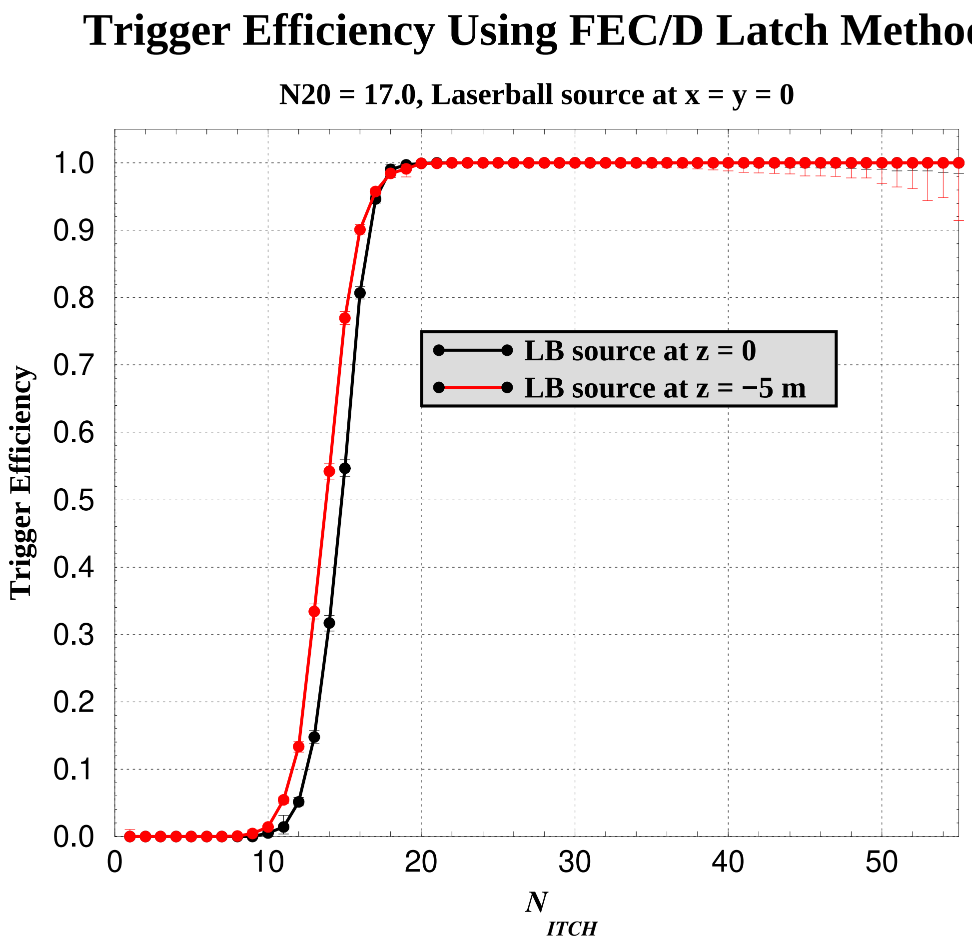

Figure 31: Measured NHIT20 trigger efficiency using the laserball with the FEC/D as the trigger latch.